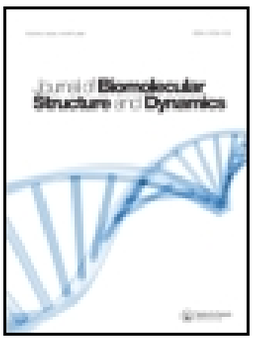

Taylor & Francis
Taylor & Francis Group

Journal of Biomolecular Structure and Dynamics

ISSN: 0739-1102 (Print) 1538-0254 (Online) Journal homepage: http://www.tandfonline.com/loi/tbsd20

Synthesis, Characterization, DNA and HSA Binding Studies of Isomeric Pd (II) Antitumor Complexes Using Spectrophotometry Techniques

Sareh Zareian-Jahromi & Hassan Mansouri-Torshizi

To cite this article: Sareh Zareian-Jahromi & Hassan Mansouri-Torshizi (2017): Synthesis, Characterization, DNA and HSA Binding Studies of Isomeric Pd (II) Antitumor Complexes Using Spectrophotometry Techniques, Journal of Biomolecular Structure and Dynamics, DOI: 10.1080/07391102.2017.1322536

To link to this article: http://dx.doi.org/10.1080/07391102.2017.1322536

Accepted author version posted online: 23 Apr 2017.

Publisher: Taylor & Francis
Journal: *Journal of Biomolecular Structure and Dynamics*
DOI: http://dx.doi.org/10.1080/07391102.2017.1322536

Synthesis, Characterization, DNA and HSA Binding Studies of Isomeric Pd (II) Antitumor Complexes Using Spectrophotometry Techniques

Sareh Zareian-Jahromi[a] and Hassan Mansouri-Torshizi*[a]

[a]*Department of Chemistry, Faculty of science, University of Sistan and Baluchestan, Zahedan, Iran,*

* Corresponding author. Tel./fax: +98-54-33431146, Fax: +98-54-33446565
E-mail: hmtorshizi@hamoon.usb.ac.ir

Synthesis, Characterization, DNA and HSA Binding Studies of Isomeric Pd (II) Antitumor Complexes Using Spectrophotometry Techniques

Sareh Zareian-Jahromi[a] and Hassan Mansouri-Torshizi*[a]

[a]*Department of Chemistry, Faculty of science, University of Sistan and Baluchestan, Zahedan, Iran,*

* Corresponding author. Tel./fax: +98-54-33431146, Fax: +98-54-33446565

E-mail: hmtorshizi@hamoon.usb.ac.ir

Abstract:

Two new Palladium(II) isomeric complexes, [Pd(Gly)(Leu)](**I**) and [Pd(Gly)(Ile)](**II**), where Gly is glycine, and Leu and Ile are isomeric amino acids (leucine and isoleucine), have been synthesized and characterized by elemental analysis, molar conductivity measurements , FT-IR, ^{1}H NMR and UV–Vis. The complexes have been tested for their *In vitro* cytotoxicity against cancer cell line K_{562} and their binding properties to calf thymus DNA (CT-DNA) and human serum albumin (HSA) have also been investigated by multispectroscopic techniques. Interactions of these complexes with CT-DNA were monitored using gel electrophoresis. The energy transfer from HSA to these complexes and the binding distance between HSA and the complexes (r) were calculated. The results obtained from these studies indicated that at very low concentrations, both complexes effectively interact with CT-DNA and HSA. Fluorescence studies revealed that the complexes strongly quench DNA bound ethidium bromide as well as the intrinsic fluorescence of HSA through the static quenching procedures. Binding constant (K_b), apparent biomolecular quenching constant (k_q) and number of binding sites (n) for CT-DNA and HSA were calculated using Stern-Volmer equation. The calculated thermodynamic parameters indicated that the hydrogen binding and vander Waals forces might play a major role in the interaction of these complexes with HSA and DNA. Thus, we propose that the complexes exhibit the groove binding with CT-DNA and interact with the main binding pocket of HSA. The complexes follow the binding affinity order of **I**>**II** with DNA- and **II**>**I** with HSA-binding.

Keywords: DNA-binding, Pd(II) complexes, Amino acids, HSA- binding, Cytotoxicity

Abbreviations:

Gly	glycine
SDS	Sodium Dodecyl Sulphate
Leu	leucine
Ile	isoleucine
CT-DNA	calf thymus deoxyribonucleic acid
EB	ethidium bromide
HSA	human serum albomine
K_{app}	apparent binding constant
K_{sv}	Stern-Volmer constant
K_b	binding constant
k_q	quenching constant
n	number of binding sites
ΔH°	enthalpy changes
ΔS°	entropy changes
ΔG°	free energy changes

1. Introduction

Medicinal inorganic chemistry plays a key role in designing the metal-based anticancer drugs which have a great interest as a potential therapeutic agent against cancer treatments (Hannon, 2007; Kostova, 2006). Yet, as a chemical agent used during chemotherapy, these drugs may cause serious side effects (Sparks & Scholz, 2009). While designing the novel therapeutic and

diagnostic metal- based anticancer drugs, the main goal is to produce new types of adducts on DNA with reduced side-effects (Erdogan & Özalp-Yaman, 2014; Singh, Joseph, Kumar, Bathini, & Lown, 1992). Recently, there has been a great interest in binding of metal complexes with DNA, for it may provide important information about new cancer therapeutic agents and potential probes of DNA structure and conformation (da Silveira et al., 2011; Gaber, El-Ghamry, & Fathalla, 2015; Li et al., 2013). Likewise, due to their promising antitumor and antibacterial activities, Pd(II) and Pt(II) complexes have attracted considerable attention in recent years (El-Shahawi, Al-Jahdali, Bashammakh, Al-Sibaai, & Nassef, 2013; Ghani & Mansour, 2012; Matesanz & Souza, 2007; Montagner, Gandin, Marzano, & Longato, 2011; Özbek, Alyar, Alyar, Şahin, & Karacan, 2013; Özdemir, Akkaya, & Özbek, 2013). Nowadays, Cisplatin (cis-$[PtCl_2(NH3)_2]$) is an important anticancer drug and its activity is related to its binding to DNA and protein (Icsel et al., 2015). This compound is used in the treatment of solid tumors (Arnesano, Losacco, & Natile, 2013; Iglesias et al., 2015); however, its use in clinical cancer settings has been limited by unwanted toxic effects, low water-solubility and acquired resistance of cancer cells. Therefore, much effort has been put forward into the development of new platinum, palladium and other metal complex-based anticancer drugs (Montana & Batalla, 2009; Ott & Gust, 2007; Zalba & Garrido, 2013). Owing to higher liability of palladium versus platinum analogs, amino acid ligands, which do not dissociate easily in aqueous solution, have been used to synthesize palladium anticancer complexes (J. Zhang, Li, Wang, Zhang, & Li, 2010). It has also been suggested that these palladium complexes may be useful for the treatment of tumors of the gastrointestinal region where cisplatin fails (Puthraya, Srivastava, Amonkar, Adwankar, & Chitnis, 1985). Recently, the metallic complexes with amino acids such as ligands have received much attention because they proved to be useful antitumoral drugs against sarcoma and leukaemia. In addition, the antibacterial agents applied against *Staphylococcus aureus*, *Escherichia coli* and *Candida albicans*, etc., were used as nutritive supplies for both human and animals (Stanila et al., 2009).

Generally, DNA is the primary intracellular target of anticancer drugs (Gumus et al., 2009). The interaction between small molecules and DNA can often manipulate biodistribution, DNA binding rate and mode. It can also be recognized by DNA-repair mechanisms, causing damage to cancer cells and blocking the division of cancer cells, and even resulting in death of cancer cells (Alagesan, Bhuvanesh, & Dharmaraj, 2014). Thus, it was thought worthwhile to study the interaction of metal-based drugs with DNA for a better understanding of their pharmacological properties and design new therapeutic agents (Katrahalli, Kalalbandi, & Jaldappagari, 2012).

Serum albumin has long been the center of attention of the pharmaceutical industry mostly because of its ability to bind with various drug molecules and to alter the overall distribution, metabolism, and efficacy of many drugs which work based on their affinity to serum albumin (Jayanthi, Anusuya, Bhuvanesh, Khalil, & Dharmaraj, 2015; Katrahalli, Jaldappagari, & Kalanur, 2010). Among the investigated proteins, human serum albumin (HSA) is the most abundant carrier protein in blood stream which has high affinity with a wide variety of ligands such as metabolites and drugs. The most important physiological functions of this protein are the storage and transport of great range of endogenous and exogenous compounds such as fatty acids, hormones, bilirubin, and drugs and the maintenance of osmotic pressure and pH of the blood plasma (Huang, Kim, & Dass, 2004; Wang et al., 2008). The crystallographic analysis of HSA revealed that this protein contains a single chain of 585 residues with a molecular mass of 66.438 kDa. It constitutes three homologous alpha-helical domains I(1–195), II(196–383) and III(384–585) that are packed in two separate sub-domains A and B. HSA contains a single Trp residue at position 214. The principal region of ligand binding on serum albumin is located between the sub-domains IIA and IIIA. The HSA/metal binding occurs mainly near Trp residue in sub-domain IIA, which has also been identified as a primary binding site for many drugs (Ascenzi & Fasano, 2010; Yousefi et al., 2015).

Several palladium (II) complexes of amino acid chelating ligands have been reported which interact with DNA and the proteins like HSA and BSA (Divsalar, Saboury, Yousefi, Moosavi-Movahedi, & Mansoori-Torshizi, 2007; Eslami Moghadam et al., 2016; J. Zhang et al., 2010). Their results suggested that the presence of different amino acids in these complexes can i) modulate their solubility ii) improve the antiproliferative properties iii) decrease structural inducing harmful efforts on the carrier proteins and iv) increase drug concentration in cancer cells. Keeping these criteria in mind, two new, water soluble, neutral and isomeric palladium (II) complexes [Pd (Gly) (Leu)](**I**)and [Pd (Gly) (Ile)](**II**), were synthesized and characterized. Their cytotoxicity against human tumor cell line K_{562} was investigated by MTT assay. The interaction of these compounds with DNA or HSA was studied by UV–Vis, fluorescence, FT-IR spectroscopy and gel electrophoresis. On the basis of the spectroscopic data, the binding parameters (K_{app}, $L_{1/2}$, K_{sv}, k_q, K_b and n), thermodynamic parameters (ΔH^o, ΔS^o and ΔG^o) and binding modes in the interaction of the Pd (II) complexes to CT-DNA and HSA were calculated. The obtained results may have important applications in drug delivery and drug design procedures.

2. Experimental

2.1. Materials and methods

All chemicals including Palladium (II) chloride, glycine, leucine, isoleucine, sodium chloride, sodium bicarbonate and Tris- HCl buffer (tris-(hydroxymethyl)methylamine) were purchased from Merck Chemical Co. and were used as received. Highly polymerized calf thymus deoxyribonucleic acid sodium salt Type 1 (CT-DNA) and Human serum albumin (HSA, free fatty acid fraction V, purity > 97%) were also obtained from Sigma–Aldrich.

FT-IR (Fourier transform Infrared) spectra of amino acids as ligands and their corresponding Pd (II) complexes were recorded on a JASCO-460 plus FT-IR spectrometer in the range of 4000 to 400 cm^{-1} in KBr pellets. The contents of carbon, hydrogen and nitrogen were determined by Herause CHNO- RAPID elemental analyzer. ^{1}H NMR (proton nuclear magnetic resonance) spectra of the compounds were recorded on a Brucker DRX- 250 Avance spectrometer at 250MHz in DMSO-d_6 (deuterated dimethyl sulfoxide) using tetramethylsilane (TMS) as the internal reference. UV-Vis (Ultraviolet- Visible) spectra of the metal complexes and ligands were further measured on a Rayligh- 1601 spectrophotometer. Melting points were measured on a Unimelt capillary melting point apparatus and were reported uncorrected. Conductivity measurements of the above Pd (II) complexes in deionized water were carried out on a Systronics conductivity bridge 305, using a conductivity cell of cell constant 1.0. Fluorescence spectra were recorded using a Cary Eclips spectrometer. Finally, the agarose gel electrophoresis was performed using gel documentation systems.

2.2. Synthesis of palladium (II) complexes

*2.2.1. Preparation of glycinatoleucinatopalladium(II), [Pd (Gly) (Leu)[(**I**):*

$PdCl_2$ (177mg, 1mmol) and NaCl (117mg, 2mmol), were added to 20mL of double distilled water. The reaction mixture was stirred for 2h at 60-70°C to yield $Na_2[PdCl_4[$. This brown solution was cooled and filtered. In the other beaker containing about 10mL of water, glycine (75mg, 1mmol) and $NaHCO_3$ (84mg, 1mmol) were mixed and stirred for 15 minutes to get sodium salt of glycine and filtered. This solution was dropletly added to the stirred solution of $Na_2[PdCl_4[$and was heated for about 2h at 50°C to get the yellow solution containing Na[Pd (Gly) (Cl_2)] and finally, it was filtered. In another beaker, leucine (131mg, 1mmol) and $NaHCO_3$(84mg, 1mmol) were dissolved in 20mL water and were stirred at 40°C for 10min to convert the leucine into its sodium salt. Then, this solution was slowly added to the above solution containing Na[Pd (Gly) (Cl_2)]. The reaction mixture was stirred at 40°C for 2h and was concentrated to 20mL to give cream colored precipitate of the desired complex. It was then

filtered and washed with water, acetone and was dried at 50°C in an oven overnight. Its yield was 217.7mg (70%). It decomposes at 210- 212ºC. Elemental analysis was also calculated for $C_8H_{16}O_4N_2Pd$ (311): C, 30.86; H, 5.14; N, 9.00. Found: C, 30.87; H, 5.13; N, 9.10.

2.2.2. Preparation of glycinatoisoleucinatopalladium(II),]Pd (Gly) (Ile)] ***(II)****:*

This neutral complex was synthesized and isolated following the procedure as given for]Pd (Gly) (Leu)[complex except that instead of leucine, isoleucine (131mg, 1mmol) was used. Its yield was 192.8mg (62%). It decomposes at 203-206ºC. Elemental analysis was also calculated for $C_8H_{16}O_4N_2Pd$ (311): C, 30.86; H, 5.14; N, 9.00. Found: C, 30.85; H, 5.15; N,9.12.

2.3. Cytotoxic Studies

2.3.1. Cell Culture

The chronic myelogenous leukemia cell line, K_{562}, was obtained from the Cell Bank of Pastor Institute of Biochemistry and Cell Biology (Iran). The cells were grown in the RPMI medium. This medium was supplemented with L-glutamine (2mM), Streptomycin and penicillin (5 µg/mL) and 10% heat-inactivated fetal calf serum at 37ºC under a 5% CO_2/95% air atmosphere (Divsalar, Razmi, Saboury, Mansouri-Torshizi, & Ahmad, 2015).

2.3.2. Cell Proliferation Assay

The above Pd (II) complexes inhibit the growth of chronic myelogenous leukemia cell line, K_{562}. This growth inhibition was measured by means of MTT (3- (4, 5-dimethylthiazol)- 2,5-diphenyltetrazolium bromide) assay. The cleavage and conversion of the soluble yellowish MTT to the insoluble purple formazan by active mitochondrial dehydrogenase of living cells has been used to develop an assay system which was an alternative to other assays for measurement of cell proliferation. Harvested cells were seeded into 96-well plate (1×10^4cell/mL) with varying concentrations of the sterilized Pd(II) complexes (0-250µM) and were incubated for 24h. Four hours to the end of incubations, 25µL of MTT solution (5mg/mL in PBS) was added to each well containing fresh and cultured medium. At the end, the insoluble formazan produced was dissolved in a solution containing 10% SDS and 50% DMF (left for 2h at 37ºC in dark conditions) and the optical density (OD) was read against a reagent blank with multi-well scanning spectrophotometer (ELISA reader, Model Expert 96, AsysHitchech, Austria) at the wavelength of 570nm. The OD value of the study groups was divided by the OD value of the untreated control and was presented as the percentage of control (as 100%) (Divsalar et al.,

2015). The 50% cytotoxic concentration (Cc_{50}) of each compound was determined from the plot of % cell growth versus [complex] for each sample.

2.4. DNA/HSA Binding studies

2.4.1. Electronic absorption spectroscopy

All the experiments involving interaction of the pd(II) complexes with DNA or HSA were carried out in a Tris-HCl buffer (5mM Tris- HCl, 50mM NaCl and pH 7.2).The stock solutions of DNA (4mg/mL), HSA (2mg/mL), and each of the synthesized Pd(II) complex (10^{-4}M) were freshly prepared in the Tris buffer. The concentrations of DNA and HSA were determined by using the extinction coefficients of DNA, $6600M^{-1}cm^{-1}$ at 260nm (Jayanthi et al., 2015) and HSA, $36500M^{-1}$ cm^{-1} at 280nm (Yousefi et al., 2015). A solution of CT-DNA gave a ratio of UV- Vis absorption at 260nm and 280nm of about 1.7–1.9, indicating that the CT-DNA was sufficiently free of protein (Annaraj, Balakrishnan, & Neelakantan, 2016; Raman & Raja, 2007). Two experiments were performed to investigate the interactions of complexes **I** and **II**, with DNA and HSA using an electronic absorption spectroscopy in the UV-Vis region.

First: a fixed amount of DNA (25µL stock solution +1.975mL Tris-HCl buffer, i.e. 0.18mM) and/or HSA (100µL stock solution +1.9mL Tris-HCl buffer, i.e. 0.013mM) was titrated separately by each metal complex (0.000- 0.042mM for DNA and 0.000- 0.040mM for HSA) at 300K. After each addition of the complex fraction, the solutions (DNA-complex / HSA-complex) were incubated for 5 min, and then the absorption spectra were recorded as 200-350nm for DNA and 230-350nm for HSA. The titration processes were continued until no change was observed in the absorption spectra. The absorption data were analyzed using Eq.(1)(Abu, Ghithan, Darwish, & Abu-Hadid, 2012).

$$\frac{1}{A-A_0} = \frac{1}{A_\infty - A_0} + \frac{1}{K_{app}(A_\infty - A_0)[metal\ complex]} \quad (1)$$

where A_0 is the initial absorption of DNA or HSA at 260 or 280nm respectively in the absence of metal complexes, A_∞ is the final absorption of the ligated DNA or HSA (i.e. when all binding sites on DNA or HSA were occupied by the desired metal complex), and A is the recorded absorption at various concentrations of metal complexes. The double reciprocal of $1/A - A_0$ vs. 1/[metal complex] is linear and the apparent binding constant (K_{app}) can be calculated from the ratio of the intercept to the slope.

In the above experiments, the selected spectra were overlaid to see if there is any isosbestic points and or hypo-, hyper-, hypso- and batho-chromic shifts.

Second: In this experiment, the conformational changes of the native CT-DNA and HSA induced by the complexes **I** or **II** were measured as a function of spectral changes (Mansouri-Torshizi, Eslami-Moghadam, Divsalar, & Saboury, 2011). Here, a constant parameter, $L_{1/2}$, i.e. the concentration of each metal complex at midpoint transition of CT-DNA or HSA from native to unfolded was determined (Mansouri-Torshizi, Mahboube, Divsalar, & Saboury, 2008).The sample cell was filed with 1.8mL of 0.17mM DNA solution (1.775mL Tris-buffer + 0.025mL stock solution of DNA) or 1.8mL of 0.014mM HSA solution (1.7mL Tris-buffer + 0.1mL stock solution of HSA). However, the reference cell was filled with 1.8mL of Tris-buffer only. Then, both cells were kept at the constant temperature of 300K or 310K, and 10µL stock solution of either Pd(II) complex was added to both cells. After a 5-min incubation, the absorption was recorded at 260nm for DNA, or 280nm (denoted A_m) and 640nm (denoted A_{640}) for HSA (Aminzadeh, Mansouri-Torshizi, & Modarresi-Alam, 2016; Islami-Moghaddam, Mansouri-Torshizi, Divsalar, & Saboury, 2009). Addition of Pd (II) complex to both cells was continued until no further change in the absorption readings was observed. As a result, the data obtained from this experiment are: A_m, A_{640}, $[L]_t$ and $a=V_2/V_1$ (where, a is dilution coefficient, V_2 is total volume of solution in the sample cell after each addition of Pd(II) complex, V_1 is initial volume, i.e. 1.8mL, and $[L]_t$ is total concentration of Pd(II) complex in each time of addition). On plotting a (A_m-A_{640}) against $[L]_t$, two types of sigmoidal plots (ascending or descending) may result. From these plots, the concentration of each metal complex at midpoint of transition, $L_{1/2}$, could be deduced for both temperatures, 300K and 310K, separately.

2.4.2. Fluorescence spectra

Fluorescence titration is one of the helpful method used for finding the interactions of metal complexes with the biomacromolecules such as DNA, HSA, BSA,…etc. The relative binding propensity of the Pd(II) complexes to DNA or HSA was studied by the fluorescence titration method. In these experiments, the excitation wavelengths of 471nm and 295nm were selected for DNA and HSA, respectively. The emission spectra were recorded from 525 to 725nm and from 300 to 500nm for DNA and HSA binding, respectively. Measurements were made using a 1cm path length fluorescence cuvette. The band slits for both excitation and emission were 5nm. The maximum fluorescence intensity was used in order to calculate the thermodynamic parameters. In the interaction studies between the above-mentioned Pd(II) complexes and DNA or HSA, the following procedures were carried out:

(i) DNA interaction studies:

The fluorescence intensity of the solutions of calf thymus DNA was checked and their emission intensities were found to be very small and negligible. Thus, ethidium bromide (EB) was used to probe the course of the interaction. In this experiment, in a quartz cell containing 1ml Tris-HCl buffer of pH=7, 25µL of DNA (stock solution) and 68µL aqueous EB (0.023mg/mL) were added and the volume was adjusted to 2mL by the same buffer. In these solution mixtures, the fluorescence of EB enhanced about 50 fold at ~ 600nm as it intercalates between the base pairs of DNA double helix (Saeidifar et al., 2014; Shahraki et al., 2014). Next, the effects of each palladium (II) complex on the emission intensity of interacted DNA-EB were studied by adding increasing concentrations of each metal complex (10-100µL of the stock solution).After each addition step and equilibration for 5min, an emission spectrum was recorded between 525 to 725nm. At the end of the experiment, all spectra were overlaid to observe the changes in their emission intensities. This experiment was performed separately for complexes **I** and **II** at three different temperatures of 293, 300, and 310K. To analyze the interaction of DNA and synthesized compounds, the quenching constant, K_{sv}, was determined by using Stern–Volmer equation (2) (Khosravi & Mansouri-Torshizi, 2017; Niroomand, Khorasani-Motlagh, Noroozifar, & Moodi, 2012).

$$\frac{F_0}{F} = 1 + K_{SV}[Q] = 1 + k_q \tau_0 [Q] \qquad (2)$$

where, F_0 and F are the fluorescence intensities of DNA-EB in the absence and presence of various concentrations of quencher, i.e. metal complex, [Q] is the total concentration of each Pd(II) complexes, τ_0 is the average fluorescence lifetime of fluorophore (in this case, EB which is 10^{-12}) in the absence of quencher and k_q is the apparent biomolecular quenching constant which equals to K_{SV}/τ_0. Therefore, the slope of the plot F_0/F versus [Q] gives the value of K_{SV} for each sample. Also, the binding constant (K_b) and the number of binding sites (n) on DNA were calculated according to Equation (3) (Icsel et al., 2015).

$$\log\left(\frac{F_0 - F}{F}\right) = \log K_b + n \log[Q] \qquad (3)$$

Here, from the plot of log (F_0-F/F) versus log [Q], the values of n and K_b could be calculated. Knowing K_b, thermodynamic parameters can be evaluated using equation (4) and Van't Hoff equation (Khorasani-Motlagh, Noroozifar, & Mirkazehi-Rigi, 2010).

$$\ln K_b = -\frac{\Delta H^\circ}{RT} + \frac{\Delta S^\circ}{R} \quad (4)$$

where K_b is the binding constant at the corresponding temperature, R represents the gas constant, T is the absolute temperature (K), and ΔH^o and ΔS^o are enthalpy and entropy changes, respectively. These two later parameters were obtained separately at 293, 300 and 310K by plotting $\ln K_b$ versus 1/T. In this plot, ΔH^o and ΔS^o were determined from the slope ($-\Delta H^o$/R) and the intercept on y axis (ΔS^o/R), respectively.

Finally, the free energy changes (ΔG^o) in the interaction between each Pd(II) complex and DNA-EB can be calculated according to Equation (5) (Khorasani-Motlagh et al., 2010).

$$\Delta G = \Delta H - T\Delta S = -RT \ln K_b \quad (5)$$

(ii) HSA interaction studies:

The procedure followed to study the interaction between HSA and each metal complex was the same as the above procedure for DNA interaction. The only difference was that there is no need of using fluorophore (EB) as in the case of DNA interaction studies. That is because HSA is intrinsically fluorescence active ($\tau_0 = 10^{-8}$). In fact, the autofluorescence activity of HSA comes from the tryptophan, tyrosine and phenylalanine residues. The intrinsic fluorescence of HSA is almost contributed to tryptophan alone, because phenylalanine has a very low quantum yield and the fluorescence of tyrosine is almost totally quenched if it is ionized or located near an amino group, a carboxyl group or a tryptophan (Abu et al., 2012). Moreover, the fluorescence activity of HSA is very sensitive to its microenvironment, and variety of molecular interactions can diminish the fluorescence intensity of this protein.

2.4.3. CT-DNA gel electrophoresis

The interactions between [Pd(Gly)(Leu)](**I**) and [Pd(Gly)(Ile)](**II**) complexes with CT-DNA were monitored using agarose gel electrophoresis on a horizontal gel apparatus. The gel was stained with EB and was photographed under UV light. In this experiment, first, a reaction mixture containing 10µL of CT-DNA (stock solution) was placed in a clean and sterile Ependorf tube and in the other 4 tubes, same amounts of CT-DNA and diverse concentrations of each Pd(II) complexes **I** or **II** (5, 10, 15 and 20µL from stock solution) were added, so, the volumes of all tubes were then increased to 40µL by Tris-HCl buffer. All tubes were mixed slowly and incubated for 1h at 310K. The reactions in the tubes were terminated by the addition of 5µL

loading buffer containing 0.25% blue bromophenol and of these mixtures, only 4µLwas finally loaded into the gel (Mohamed, Shoukry, & Ali, 2012). The product resulting from the interactions of the complexes **I** and **II** with CT-DNA electrophoresis on the agarose gel was prepared in 1% (w/v) of TAE buffer (40mMTris-acetate, 1mM EDTA)(pH=8.28) at constant voltage of 50V for 2h, until the blue bromophenol had travelled through 75% of the gel. After electrophoresis, the gel was stained for 30min by soaking in an aqueous ethidium bromide (0.5µg/mL). The gel was then destained for 10min by being kept in sterile distilled water. The interacted CT-DNA bands were visualized by viewing the fluorescence of intercalated EB under UV light, and then, were photographed. The binding ability was observed and assessed for the intensity and mobility of the bands (Shoukry & Mohamed, 2012).

2.4.4. Calculations of energy transfer

The efficiency of energy transfer (E) in biochemistry can be used to evaluate the distance between the metal complex and the fluorophores in the protein .According to Foster Resonance Energy Transfer (FRET), the efficiency of energy transfer (E) could be calculated by Eq.(6) (Matei, Ionescu, & Hillebrand, 2011):

$$E = R_0^6/(R_0^6 + r_0^6) = 1 - \frac{F}{F_0} \quad (6)$$

where F and F_0 are the fluorescence intensities of HSA in the presence and absence of metal complex, r is the distance between acceptor (bound metal complex) and donor (tryptophan residue) and R_0 is the critical distance when the transfer efficiency is 50%. The value of R_0 was calculated using the following equation (Matei et al., 2011):

$$R_0^6 = 8.8 \times 10^{-25} K^2 N^{-4} \Phi J \quad (7)$$

In the above equation, K^2 is the spatial orientation factor describing the relative orientation in space of the transition dipoles of the donor and acceptor, N is the refractive index of the medium, ϕ is the fluorescence quantum yield of the donor and J is the overlap integral of the fluorescence emission spectrum of the donor with the absorption spectrum of the acceptor which could be calculated by Eq. (8) (Matei et al., 2011):

$$J = (\Sigma F(\lambda)\varepsilon(\lambda)\lambda^4 \Delta\lambda)/(\Sigma F(\lambda)\Delta\lambda) \quad (8)$$

where F(λ) is the corrected fluorescence intensity of the donor at wavelength λ and ελ is the UV molar absorption coefficient of the acceptor at the wavelength λ. Under the experimental condition, the value of K^2 = 2/3, N = 1.336 and ϕ= 0.188(Matei et al., 2011).

2.4.5. FT-IR Spectroscopy

To further understand the structural alterations of HSA induced by binding of the isomeric Pd(II) complexes, FT-IR spectra of HSA alone, and complexes **I**- or **II**–HSA systems in the region of 1800-1400cm^{-1} in KBr pellets were recorded at room temperature. Spectra of buffer solution were collected at the same condition. Then, the absorbance of buffer solution was subtracted from the spectra of sample solution. Finally, the difference spectra of HSA were obtained by subtracting the spectrum of each metal complexes **I**- or **II**-free form from that of **I**- or **II**–HSA bound forms with the same concentrations (Yue, Chen, Qin, & Yao, 2009).

3. Results and discussion

Two new, neutral and sufficiently water soluble complexes, [Pd(Gly)(Leu)](**I**) and [Pd(Gly)(Ile)](**II**), (where Gly is glycine, Leu is leucine, and Ile is isoleucine), were prepared by interaction of Na[Pd(Gly)(Cl_2)] with an appropriate amount of leucine and isolucine sodium salts. As shown in Fig.1, since leucine and isoleucine are the only isomeric pair of amino acids among the twenty essential amino acids present in the structure of proteins, resulting Pd(II) complexes can show isomeric from this source. This is the delicacy of the present research work which has been looked at to see if there is much difference in their behaviors. The complexes were isolated as yellow solids and our attempts to make single crystal suitable for X-ray crystallography were unsuccessful.

Molar conductance of 10^{-4}M solution of complexes **I** and **II** in water were 8 and 9$cm^2.ohm^{-1}.mol^{-1}$, respectively, indicating that these Pd (II) complexes behave as non-electrolytes (Angelici, 1969).

Electronic absorption spectra of both complexes show two bands at 206nm and 320nm for complex **I** and 202nm and 318nm for complex **II** assigned respectively to π→ π* and n→ π*transition of C=O groups of amino acids(Stanila et al., 2009). However, the absorption peak of both complexes at 206nm and 202nm showed a red shift of ~14nm from more polar water to less polar methanol , indicating that this peak is not only due to π→ π* transition of amino acid ligands but also may be due to metal-ligand charge transfer overlaying each other (Cotton, Wilkinson, Bochmann, & Murillo, 1999).

Information about the metal ions coordination was obtained by comparing the FT-IR frequencies of free amino acids with their corresponding Pd(II) complexes. In the spectrum of the leucine, isoleucine and glycine the ν (N–H) stretching vibration appears at 3055, 2958 and 2900cm^{-1} respectively and are shifted in their corresponding Pd (II) complexes to 3286cm^{-1} in **I** and 3244cm^{-1}in **II** proving the involvement of the -NH_2 groups in the complex formation (Stanila et al., 2009). The absorption band at 1608cm^{-1} was attributed to the ν (C=O) stretching vibration in the spectra of the free amino acids. This band appearing at 1635cm^{-1} and 1654cm^{-1} in the spectra of **I** and **II** shows that -COO group is coordinated to the metal center (Stanila et al., 2009).

The ^{1}H NMR spectra of **I** and **II** were recorded in DMSO-d_6 using TMS as an internal reference. The proposed structures and NMR numbering schemes are given in Fig. 1. In the ^{1}H NMR spectrum of **I**, three multiple signals appeared at 0.86, 1.51, and 3.08ppm are assigned to H_a(6H), H_b; H_c (3H) and H_d; H_e (3H), respectively. The protons of NH_2 groups of glycine and leucine (4H, $H_{ff'}$) resonated as four broad signals with low intensity in the range of 4.03 to 5.25ppm. The large upfield shift of 0.62 and 0.55ppm of H_d and H_e protons as compared with H_d and H_e protons of free amino acids supports the binding of N of the -NH_2 groups and O of the -COO groups of glycine and leucine to Palladium(II) (Puthraya et al., 1985).

The ^{1}H NMR spectrum of **II** exhibits five signals at 0.87, 1.01, 1.42, 1.78, and 3.07ppm which are assigned to H_a (3H), H_b(2H), H_g (3H), H_c (1H) and H_d; H_e (3H), respectively. The protons of NH_2 groups of glycine and isoleucine (4H, $H_{ff'}$) resonate as four broad signals with low intensity in the range of 3.67 to 4.91ppm. The large upfield shift of H_d (0.92ppm) and H_e (0.55ppm) protons supports the binding of N of the -NH_2 group and O of the -COO group of these amino acids to Pd(II) (Puthraya et al., 1985).

On the basis of the above characteristic data of elemental analysis, conductivity measurements, UV-Vis, FT-IR and ^{1}H NMR spectra, the proposed structural formula of the isomeric Pd (II) complexes are given in Fig.1.

Figure.1.

In addition to the above characterization data, the results of following experiments are discussed here.

i) Cytotoxic studies. ii) Apparent binding constant (K_{app}), in the interaction of each Pd(II) complex with CT- DNA or HSA and ability of each metal complex to unfolding CT- DNA or HSA ($L_{1/2}$) by using UV- Vis technique. iii) Ethidium bromide displacement, Stern Volmer

quenching constant (K_{sv}), binding constant (K_b), number of binding sites (n), thermodynamic parameters (ΔH^o, ΔS^o and ΔG^o) and binding mode by using fluorescence technique. iv) Gel electrophoresis. V) Energy transfer by using UV-Vis and fluorescence techniques and VI) alteration of HSA secondary structure by using FT-IR technique.

3.1. Cytotoxicity tests of the Pd (II) amino acid complexes

The *Invitro* effect of the prepared complexes on human leukemia cell lines was evaluated by MTT assay. In these studies, different concentrations of the isomeric Pd (II) complexes **I** or **II** from 0 to 100μM of stock solutions were used in the culture medium of the cell line (Fig.2). The 50% cytotoxic concentration (Cc_{50}) of complexes **I** and **II** after 24h incubation time are 40μM and 50μM, respectively. As shown in Fig.2, cells growing after 24h was significantly reduced in the presence of various concentrations of the Pd (II) complexes and the Pd (II) complexes produce a dose-response suppression on growing of K_{562} leukemia cell line. Furthermore, the Cc_{50} value of cis-diamminedichloroplatinum (II), the well-known anti-cancer drug was measured under the above same experimental conditions. This value (154μM) is much higher than the Cc_{50} values of the above two Pd (II) complexes. It can be noticed that the presence of amino acids in the structure of these synthesized complexes as well as their higher water solubility (~ 60mg/mL) as compared to cisplatin (~2.53mg/mL)(Yi & Bae, 2011) might influence the anti-tumor activities of these complexes on K_{562} cell line.

Figure.2.

3.2. The UV-Vis absorption studies in the interaction between isomeric Pd (II) complexes with CT-DNA and HSA

Application of electronic absorption spectroscopy is one of the most useful techniques for probing the interactions of metal complexes with DNA and HSA, as any interaction with the macromolecule will cause electronic perturbations in them (Abdi, Hadadzadeh, Salimi, Simpson, & Khalaji, 2012). A fixed amount of CT-DNA (0.18mM) or HSA (0.013mM) was titrated by increasing the concentrations of the complexes **I** and **II** (0.000-0.042mM for DNA and 0.000-0.040mM for HSA) at 300K. The decrease in the absorption maxima of DNA (260nm) and HSA (280nm) without any obvious change in these peak positions are shown in Fig.3. These observations indicate the interaction between both Pd (II) complexes with CT-DNA and HSA molecules. There was no change in the absorption spectra if more metal complexes were injected to the systems, suggesting saturation of CT-DNA and HSA binding

sites; thus, no further interaction occurred. However, in the titration of CT-DNA and HSA with different amounts of complex **I**, two isosbestic points were observed respectively at 240 and 300nm for DNA and at 260 and 295nm for HSA systems (see Fig. 3, a and c). The presence of these isosbestic points suggest that: (i) There is an equilibrium between DNA and or HSA bound and free forms of metal complex **I** and these two forms have same absorption at the isosbestic points (Huheey, Keiter, & Keiter, 1983) (ii) A good indicator of there being only two absorbing species in solutions, and the final spectrum corresponding to that of interacted CT-DNA-Pd or HSA-Pd complex, and (iii) Two isosbestic points indicate that the reaction proceeds without any side reactions (such as hydrolysis). Utilizing Eq. (1), the overall binding constant of complexes **I** and **II** to CT-DNA and HSA were estimated. In the plot of $1/ (A - A_0)$ vs. 1/[metal complex], the apparent binding constant (K_{app}) can be obtained from the ratio of y intercept to slope (see Fig.3 insert). The values are given in Table 1.

Table 1:

These K_{app} in the interaction of these complexes with CT-DNA are lower than those reported for classical intercalator such as Ethidium bromide and [Ru(phen)DPPZ] whose binding constant has been found to be in the order of 10^6-10^7M(Xu, Chen, Xi, Liu, & Zeng, 2008). These results suggest the binding modes of the complexes to CT-DNA should be non-intercalation and differ from that of EB and [Ru(phen)DPPZ]. Moreover, binding with DNA via intercalation usually results in hypochromism and bathochromism of the absorption. This is due to a consequence of strong π-π* staking interaction between planar aromatic moiety of the complexes and DNA base pairs (Chaveerach, Meenongwa, Trongpanich, Soikum, & Chaveerach, 2010). These results are in agreement with the proposed structure of the complexes **I** and **II** having no planar aromatic moieties to act as intercalator.

Figure.3.

3.3. Determination of concentrations of metal complexes in midpoint transition, $L_{1/2}$.

The profiles of the conformational changes in the structure of native CT-DNA or HSA which were induced by complexes **I** and **II** are shown in Fig. 4. These conformational changes occurred in such a manner that the absorbing groups of DNA (purine and pyrimidine bases) and HSA (mainly tryptophan residues) get hidden from UV light, resulting in a decrease in the intensity of the absorption peak with an increase in the concentration of Pd(II) complexes at the same wavelength. Thus, the native and interacted CT-DNA or the unloaded and loaded HSA by

any of synthesized Pd(II) complexes have different conformations, so the transition between these two conformations is discussed under the above title. The concentration of both Pd(II) complexes in the midpoint transition, $L_{1/2}$, was needed for transition of the native to the interacted CT-DNA or the unloaded to loaded HSA at 300 and 310K is quite low (see Fig. 4 and Table 1). This is one of the most important observations made in this research work, since a lower side effect may be observed in the case of compounds having activity at lower concentration (Edwards & Aronson, 2000). Looking at $L_{1/2}$ values given in Table 1, the following points could be deduced: (i) $L_{1/2}$ values of CT-DNA are lower than those of HSA indicating that the complexes show more interaction affinities towards DNA than with HSA. This is expected because there may be more available binding sites on DNA as compared with those of HSA. (ii) $L_{1/2}$ values of CT-DNA and HSA at 300K are lower than those of 310K. The results indicated that the reaction between the Pd(II) complexes with CT-DNA and HSA may be exothermic and (iii) In the interaction between complex **I** with CT-DNA, $L_{1/2}$ values at temperatures of 300 and 310K, are lower than those for complex **II** suggesting that the interaction affinity of the complex **I** is more than that of complex **II**. However, in the interaction between the complex **II** with HSA, $L_{1/2}$ values in both temperatures of 300 and 310K, are lower than those for the complex **I** suggesting an interaction affinity of the complex **II** with HSA is more than that of the complex **I**. Similar results have also been reported for the complex [Pd (Hex-dtc) (phen)]NO_3 (Mansouri-Torshizi et al., 2011).

Figure.4.

3.4. Fluorescence experiments with calf thymus DNA

In order to gain further support for the interaction mode between the metal complexes and DNA, we have also performed a fluorescence titration experiment(Abdi et al., 2012). It is well known that small molecules can bind to DNA through four major modes of interactions: covalent-, intercalation- , surface-, and groove-binding (Khorasani-Motlagh et al., 2010). In the case of covalent binding, there should be a labile ligand (generally monodentate) coordinated to the central metal ion of the complex to be substituted by a nitrogen base of DNA such as guanine N7 which is a well-known binding type of cisplatin (Bobek et al., 2006). This type of binding may not be possible in our cases, since both ligands around Pd (II) center are coordinated as bidentate chelate and cannot be easily replaced (see Fig.1). Intercalation of a ligand between DNA base pairs causes DNA to be lengthened and bent, while highly charged cations, such as cobalt(III) and polyamines induce condensation through charge neutralization of backbone

phosphate groups (Khorasani-Motlagh et al., 2010). Considering the structures of two new isomeric metal complexes)see Fig.1), intercalation of these compounds between base pairs of DNA may not be in favor, since there are no aromatic and planar moieties present in the structures of the Pd(II) complexes. The surface binding which is mainly consisted of electrostatic attraction and hydrogen bonding is proposed as the primary factors for the sequence specific groove binding from the theoretical analysis. As shown in Fig.1, both complexes reported here are neutral, so the possibility of electrostatic binding between these complexes and CT-DNA is nil. Therefore, we expect groove binding through other forces such as H-binding and Van der Waals forces being the major forces acting between complexes **I** or **II** with CT-DNA. This type of interaction is further supported by the following experiments.

3.4.1. Competitive DNA-binding studies with EB

To further investigate the interaction between the synthesized metal complexes and DNA, a competitive binding assay was carried out between Ethidium bromide and each Pd (II) complex with DNA. EB is a known DNA intercalator which inserts itself between the base pairs in the double helix and forms soluble complexes with nucleic acids. The fluorescence intensity of EB is very weak in aqueous solution, but its intensity increases ~50-fold in the presence of DNA (Saeidifar et al., 2014; Shahraki et al., 2014). When a metal complex which could bind to DNA more strongly than EB was added to a solution containing the EB–DNA system, the fluorescence quenching of EB–DNA is observed. The competitive binding studies involve an addition of Pd(II) complexes to DNA incubated with EB ([DNA]/[EB] = 30) and then measuring the emission intensities of the EB– DNA system. As shown in Fig. 6, the emission intensity of DNA–EB at 600nm decreased with addition of different amounts of each Pd (II) complex to be interacted DNA-EB. The observed quenching of the DNA–EB fluorescence intensity suggests that these complexes can displace EB from the DNA–EB system (Anjomshoa, Fatemi, Torkzadeh-Mahani, & Hadadzadeh, 2014). Also, the experiment revealed that addition of the complexes **I** or **II** to DNA bound EB does not cause releasing EB molecules, while the emission intensity decreases steadily. In case of EB release, a weak intensity spectrum due to free EB near the base line should appear which has not been observed in our cases (see Fig. 5). This implies that the two probes, the complexes and EB, probably bind independently with DNA and at the same time, binding of each complexes **I** or **II** affects the binding of the EB by slight slip out of EB from hydrophobic to hydrophilic regions diminuendo in emission intensities. Thus, this experiment supports the above groove binding expectation(Khorasani-Motlagh et al., 2010).

Figure. 5.

3.4.2. Stern-Volmer quenching constants

Titration of CT-DNA-EB with various amounts of complexes **I** or **II** was quantified by measuring the fluorescence quenching of the CT-DNA-EB solution. In fact, two quenching processes are known: static and dynamic. Dynamic quenching or collisional quenching requires the contact between the excited lumophore and the quenching species, the quencher. The rate of quenching is diffusion controlled and depends on temperature and viscosity of the solution. The quencher concentration must be high enough, so the probability of collision between the analyte and quencher is significant during the lifetime of the excited species (Kashanian, Khodaei, & Pakravan, 2010). The other form of quenching is static quenching in which the quencher and the fluorophore in the ground state form a stable complex. Dynamic and static quenching can also be discerned by their differing dependence on temperature**.** Dynamic quenching depends upon diffusion. Since higher temperatures lead to larger diffusion coefficients, the K_{sv} can be increased by raising the temperature. In contrast, this increased temperature is likely the result of decreased complex stability, and, thus, lower static quenching constant is resulted (Baguley & Le Bret, 1984). In order to clarify the quenching mechanism of CT-DNA-EB by complexes **I** and **II**, the Stern-Volmer (Equation (2)) is used to analyze the fluorescence quenching data. This equation has been explained in the experimental section. The K_{sv} values for the above Pd(II) complexes are obtained from the slope of the plot F_0/F versus [Q] at three temperatures. According to the classified Stern-Volmer equation, the quenching plots (Fig.6) illustrate that the quenching of EB bound to DNA by the complexes are in good agreement with the linear Stern-Volmer equation (Derakhshankhah et al., 2012). Finally, the K_{sv} and k_q at different temperatures were obtained. The results are shown in Figure 6 and Table 2.

Table 2:

In Table.2, the results show that the values of K_{sv} and k_q decrease with increasing of the temperature and the values of k_q is greater than $2.0\times10^{10}Lmol^{-1}S^{-1}$, which indicates that the probable quenching mechanism of DNA-EB solution is a static quenching (Hussein, 2011; Shaikh, Seetharamappa, Kandagal, & Manjunatha, 2007). Similar results have also been reported by A. Heydari, et. al. for [Pd(acac)(Ala)] complex(Heydari & Mansouri-Torshizi, 2016).

Figure.6.

3.4.3. Binding constant (K_b) and binding stoichiometry (n)

Fluorescence titration data were used to determine the binding constant (K_b) and the number of binding sites (or the binding stoichiometry) (n) for the complex formation of CT-DNA-EB with complexes **I** or **II** (Kashanian et al., 2010). Based on Equation (2), the values of K_b and n were determined from the intercept and slop of ($\log[(F_0\text{-}F)/F]$ versus log [Q], respectively (Fig.7). These corresponding calculated results are listed in Table 2. Data on Table 2 show that the values of K_b decrease with increasing of temperature, indicating that the stability of DNA-EB complex reduces as the temperature rises. The number of binding sites *n* is approximately equal to unity, indicating that there is one independent class of binding sites on DNA for each Pd(II) complex. Similar observations were made for the reported metal complex (Ahmadi, Alizadeh, Shahabadi, & Rahimi-Nasrabadi, 2011; Mukherjee et al., 2013). However, the values of n and K_b which decrease with rises in temperature demonstrate that the complex formation between CT-DNA-EB and Pd(II) complexes can be regarded to be an exothermic procedure. Finally, the values of K_b had a trend similar to the K_{app} values (Table1) for title complexes and values of K_b represent lower binding affinity of complex **II** to DNA than complex **I**. This is a noticeable point which might be due to the difference between leucine side chain ($\text{-}CH_2\text{-}CH(CH_3)_2$) and isoleucine side chain ($\text{-}CH(CH_3)\text{-}CH_2\text{-}CH_3$) which also plays an important role in the above interactions.

Figure. 7.

3.4.4. Thermodynamic studies

To have a better understanding of thermodynamic of the complication reaction between isomeric complexes **I** or **II** and DNA-EB, contributions of enthalpy and entropy should be determined in the reaction. Thermodynamic parameters describing the binding reactions can be divided into three contributions. The first contributions are due to the hydrogen bonding and the hydrophobic interactions between the Pd(II) complexes and CT-DNA-EB-binding sites. The second contribution arises from the conformational changes in either the nucleic acid or the complexes **I** or **II** upon binding. The third contributions are provided by the coupled processes such as ion release, proton transfer, or changes in the hydration water. Evaluation of the formation constant for the each Pd(II) compound- DNA-EB complex at three different temperatures (293, 300 and 310K) allows thermodynamic parameters of **I-** or **II**–DNA formation to be determined via Van't Hoff equation (Eq. 4). By plotting $\ln K_b$ versus 1/T (Fig. 8), ΔH^o and ΔS^o were determined (Kashanian et al., 2010). Knowing these two values, ΔG^o was

calculated from the following standard equation (Eq. 5).Thus, according to Eqs. (4) and (5), the obtained values of ΔH^o, ΔS^o and ΔG^o and the results are shown in Table 3.

Table 3:

Generally, the intercalation interactions are driven by a large favorable enthalpy reduction and an unfavorable entropy decrease, but the groove binding reactions are mostly driven entropically. The electrostatic interactions exhibit small or zero enthalpy and positive entropy changes, but hydrogen bonding and Van der Waals interactions are usually along with negative ΔH^o and ΔS^o. However, the hydrophobic interactions are characterized by positive entropy and enthalpy changes (Niroomand et al., 2012). Considering the thermodynamic parameters given in Table 3, the binding forces are spontaneous because the Gibbs free energy change value is negative. It is also demonstrated that both enthalpy and entropy changes are negative, suggesting that the Pd(II) complexes were hold in DNA grooves via hydrogen and Van der Waals binding. It could also be explained that, owing to the binding of complexes to DNA, some conformational changes may induce the results to the partial destacking of some base pairs. It was showed by the decrease in fluorescence emission intensity of DNA-EB upon addition of the Pd (II) complexes. These results are quite in agreement with the proposed structures of the Pd (II) complexes (Fig.1). As shown in Figure 1, the carbonyl and -NH_2 groups of amino acids coordinated to Pd (II) center are susceptible for H-binding and –CH_2-$CH(CH_3)_2$ group of leucine and –$CH(CH_3)$-CH_2-CH_3 group of isoleucine can interact via Van der Waals forces in groove binding. Moreover, the negative values of ΔH^o indicate that the above interaction proceeds exothermically.

Figure. 8.

3.5. Fluorescence experiments with Human Serum Albumin (HSA)

In order to determine the quenching mechanism of the interaction between HSA and the synthesized isomeric Pd(II) complexes, the fluorescence experiments were carried out at three different temperatures (293, 300 and 310K). The fluorescence emission spectra of HSA in the absence and presence of different concentrations of the Pd (II) complexes at 293K are shown in Figure 9.

Figure. 9.

As shown in this figure, the HSA fluorescence intensities were gradually decreased by increasing the concentration of each Pd(II) complex, indicating that the Trp residue was transferred into a more hydrophobic environment during the interaction. The similar emission profiles were observed as the experiments were repeated at 300 and 310K (Yousefi et al., 2015). In later parts of these studies, it was observed that the number of binding sites for each metal complex per HSA molecule equals unity, i.e., there is only one binding site for each Pd(II) complex on HSA and once it gets occupied, no further change was observed in the emission spectrum, suggesting that the interaction between each neutral Pd(II) complex and HSA includes the occupation of one binding site. Probably, there are no more interactions with other parts of HSA molecule causing structural damage to bring about possible side effects in the physiological systems (Mansoori-Torshizi, Islami-Moghaddam, & Saboury, 2003). This is in fact the normal function of the protein HSA in the blood stream that should transfer the drug agents without damaging itself.

For better quantitative understanding of the magnitude of the complexes to quench the emission intensity of HSA (see Fig. 9), Stern-Volmer Eq.(2) can be used. A plot of F_0/F against the concentration of complexes **I** and or **II** results in liner plots (Fig. 10) and the K_{sv} values are obtained from the slopes. The observed K_{sv} values indicated good HSA binding affinities of the two complexes, but the complex **II** exhibited a higher protein binding ability (Table 4).

Table 4:

The k_q values for complexes **I** and **II** are $0.32\times10^{12}M^{-1}S^{-1}$ and $0.42\times10^{12}M^{-1}S^{-1}$ at 300K, respectively. From the other side, k_q of various quenchers with biopolymers is $2.0\times10^{10}Lmol^{-1}S^{-1}$ (Lakowicz & Weber, 1973). Thus, the calculated k_q in the protein quenching procedure is greater than the maximum scatter collision-quenching constant of biopolymers. This indicated that a static quenching mechanism is operating (Anbazhagan & Renganathan, 2008; Banerjee, Ghosh, Sarkar, & Bhattacharya, 2011). Moreover, the curves F_0/F versus [Q] which are linear support the static quenching, too.

Figure. 10.

The binding constant, K_b, of the quenchers (**I** and **II**) with HSA and the number of binding sites, n, on HSA available for the complexes **I** and **II** were calculated using Eq. (3) (Table 4). The K_b values were determined from the slope of plot log (F_0-F/F) versus log [Q] (Fig. 11). The results are consistent with greater binding affinity of complex **II** as compared to that of complex **I**.

Similar results were obtained for the reported metal complexes (Jin et al., 2015; L.-W. Zhang, Wang, & Zhang, 2007). The same observations were made in the UV-Vis absorption experiments (K_{app} value of **II** is greater than that of **I**). The values of n for both complexes at the experimental temperatures approximately equal to 1, indicating that there is just a single binding site on HSA for each Pd (II) complex. As the complexes are natural, they most likely bind to the hydrophobic pocket in the sub-domain IIA of HSA. The above observations have been made by A. Heydariet. al.(Heydari & Mansouri-Torshizi, 2016).

Figure. 11.

By plotting the binding constants, K_b, from Table 4, versus temperatures and using Eqs. (4) and (5), the thermodynamic parameters were obtained (Fig. 12). The calculated enthalpy, free energy, and entropy changes are summarized in Table 5. In this study, the negative values of ΔG^o indicated that the interaction of **I** and **II** with HSA are spontaneous. On the other hand, the negative values of ΔH^o and ΔS^o suggested that hydrogen bond and Van der Waals interactions are involved in the binding of these two Pd(II) complexes with HSA. Therefore, these two forces may play a main role in holding Pd(II) complexes in the hydrophobic pocket located in the sub- domain IIA of HSA molecule (Bi et al., 2005).

Table 5:

Figure. 12.

3.6. Interaction of CT-DNA with complexes I and II by DNA mobility shift experiments in agarose gel electrophoresis

Gel electrophoresis is a technique that works on the migration of DNA in the agarose gel under the influence of electric potential as a function of their mass, charge and shape (Budagumpi, Kulkarni, Kurdekar, Sathisha, & Revankar, 2010). Here, several gel electrophoresis studies were done to unravel the effects of the new synthesized compounds **I** and **II** on CT-DNA. In these experiments, changes in electrophoretic mobility of CT-DNA in absence and presence of metal complexes are usually taken as the evidence of metal complex- DNA interaction. Retardation of the electrophoretic mobility of a DNA band could be attributed to the binding of certain molecules of the compound able to increase its molecular weight, while precession of the electrophoretic mobility could be attributed to the degradation (or damage) of the initial DNA substrate, mirrored to a decrease in its molecular weight. DNA molecules with molecular

weights lower than those of the initial DNA molecule derived from DNA breakage effect migrate faster, while DNA molecules with higher molecular weight delay more than the mobility of the initial DNA (Protogeraki et al., 2014). In other words, the larger the retardation of DNA, the greater the DNA unwinding (or interaction) produced by the given compound(Fox, 1997). However, depending on the type of DNA, the interaction of metal complex with DNA may decrease or increase the mobility. For instance, binding of cisplatin to plasmid DNA results in a decrease in mobility of supercoildplasmid DNA (Form I) and an increase in mobility of the open circular plasmid DNA (Form II). The ability of complexes **I** and **II** to interact with double stranded CT-DNA were investigated using an electrophoretic analysis through the examination of the effect of different concentrations of new Pd(II) complexes **I** and **II** (1.25, 2.50, 3.75 and 5.00mM) on the DNA. As shown in Fig. 13, with an increase in the complex concentration, the intensity of CT-DNA band decreased as compared to the band of free CT-DNA. This decrease in the intensity of the bands is believed to be due to the quenching fluorescence of CT-DNA-intercalated Ethidium bromide by increasing concentrations of Pd(II) complexes. These observations are in agreement with the observed static quenching of DNA-EB by these two complexes upon interaction via the groove binding. It has been reported that such a groove binding may bring about conformational changes resulting in partial slip of intercalated EB from hydrophobic to hydrophilic moieties and a decrease in fluorescence intensity (Khorasani-Motlagh et al., 2010). Moreover, a small up-shift in the mobility of the bands was recorded for both complexes **I** and **II** after binding to CT-DNA as compared to free CT-DNA. This delay in the electrophoretic mobility of the bands was barely visible at the bottom of the bands, leading to the formation of V letter by connecting bottom tip portions of all bands. The delay in the electrophoretic mobility of the bands may be explained by the bases of binding of the Pd (II) complexes to CT-DNA increases its molecular mass. It could also be attributed to changes in conformation of CT-DNA due to its binding with metal complexes (Fox, 1997).

Figure. 13.

The above observations converge towards the conclusion that both complexes **I** and **II** bind to CT-DNA and this result is in accordance and reinforces the view expressed by the spectroscopic experiments, which refer to the potential modes of binding with CT-DNA.

3.7. Energy transfer between complexes I and II with HSA

The energy transfer efficiency and distance between the synthesized Pd (II) complexes and HSA can be estimated using Forster's Resonance Energy Transfer (FRET) theory. FRET is a distance

dependent interaction in which excitation energy is transferred nonradiatively from a donor (Trp214 residue of HSA) to an acceptor molecule (here complexes **I** or **II**), with the prerequisite that a non-zero overlap exists between the emission spectrum of the donor and the absorption spectrum of the acceptor, which is fulfilled for the HSA–**I** /-**II** pair (Fig. 14) (Matei et al., 2011). The rate of energy transfer depends on: (i) the extent of overlapping between fluorescence emission spectrum of donor and the absorption spectrum of acceptor, (ii) the relative orientation of the donor and acceptor dipoles, and (iii) the distance between the donor and the acceptor (Tabassum, Al-Asbahy, Afzal, & Arjmand, 2012). From Eqs. (6)– (8), the values of r, R_0, J and E were calculated (Table 6). The average distance of 2–8nm between a donor and acceptor pair indicates that the energy transfer from HSA to metal complexes occurs with high probability. As can be inferred from results, the values of r suggest that the energy transfer from HSA to the synthesized Pd (II) complexes can occur with high probability.

Table 6:

Figure. 14.

3.8. Changes of the protein's secondary structure induced by metal complexes binding

FT-IR spectroscopy is a helpful technique for the study of hydrogen bonding and has been identified as one of the few techniques that are established in the determination of protein secondary structure at different physiological systems. The information on the secondary structure of proteins arises from the amide bands which result from the vibrations of the peptide groups of proteins. When small molecules bind to a globular protein like HSA, changes in the hydrogen bonding which is involved in the peptide linkages would occur, resulting in changes in the vibrational frequency of the different amide modes. The modes most widely used in the protein structural studies are amide I, amide II, and amide III. Amide I band ranges from 1600 to 1700cm^{-1} and arises principally from the C=O stretching. Amide II band is primarily an N-H bending with a contribution from C-N stretching vibrations, and ranges from 1480 to 1600 cm^{-1}. Amide III band ranges from 1220 to 1330cm^{-1} because the C-N stretching mode coupled to the in-plane N-H bending mode (Abu et al., 2012; Neault & Tajmir-Riahi, 1998). Fig. 15 shows the FT-IR spectrum of free HSA and Pd(II) complex-bound form of HSA with its difference spectrum of these two. The spectrum in Fig. 15(a) was obtained by subtracting the FT- IR absorption of the Tris–HCl buffer from the spectrum of the protein solution. The spectrum in Fig. 15(b) was obtained by the FT- IR absorption of Pd (II) complex was bounded to HSA and

the spectrum in Fig. 15(c) was obtained by subtracting the FT- IR absorption of the Pd(II) complex-free form from that of the Pd(II) complex-bound form. As shown in Fig. 15, the peak position of amide I bands has changed from 1657.12 to 1659.78cm^{-1} and 1657.12 to 1664.76cm^{-1} for complexes **I** and **II,** respectively, which indicated that the secondary structure of the protein has been changed after Pd (II) complexes were interacted. These results also indicated that these synthesized Pd (II) complexes interacted with the C=O and C–N groups in the protein polypeptides. This is in accordance with H- bonding results obtained from fluorescence studies. The HSA–Pd (II) complexes caused the rearrangement of the polypeptide carbonyl hydrogen bonding network, and finally, the reduction of the protein α-helical structure. Similar observations were made by S. Shahrakiet. al. (Shahraki, Shiri, Mansouri-Torshizi, & Shahraki, 2016).

Figure. 15.

4. Conclusion

In summary, we have designed and prepared two new, water soluble, neutral, and isomeric Pd(II) complexes, [Pd(Gly)(Leu)](**I**) and [Pd(Gly)(Ile)](**II**) (Gly, Leu and Ile are glycine, leucine and isuleucine amino acids, respectively). Their molecular structures were characterized by elemental analysis, conductivity measurement, FT-IR, UV-Vis and ^{1}H-NMR techniques. Structural studies showed that amino acids coordinated as bidentate chelate with the Pd(II) center (Fig.1). The *Invitro* cytotoxic activities were studied by MTT assay against the cancer model's cell line K_{562}, indicating that isomer **I** is more active than that of **II**, but both have good activity potential and possible future improvements. The interactions of these water soluble complexes with CT-DNA and HSA were carried out by using absorption spectroscopy, fluorescence titration spectra, Ethidium bromide titration, and gel electrophoresis studies. The results suggest that: i) both isomeric complexes exothermically interact with CT-DNA and HSA at very low concentrations, ii) interaction affinity of isomer **I** to DNA is more than that of isomer **II** and the reverse was observed for HSA interaction, iii) thermodynamic parameters indicated that **I** and **II** spontaneously interact with CT-DNA by groove binding and probably get loaded in main binding site of HSA via H-binding and Van der Waals forces, iv) quenching mechanism of both CT-DNA-EB and HSA solutions by the isomeric Pd(II) complexes seems to be statically quenching, and v) number of binding sites for both **I** and **II** on CT-DNA and HSA is approximately equal to unity. On the basis of the above results, it was concluded that these types of isomeric complexes may be useful in development of drug formulation.

Acknowledgment

Funding of our research from the university of Sistan and Baluchestan (USB) is gratefully acknowledged.

References

Abdi, K., Hadadzadeh, H., Salimi, M., Simpson, J., & Khalaji, A. D. (2012). A mononuclear copper (II) complex based on the polypyridyl ligand 2, 4, 6-tris (2-pyridyl)-1, 3, 5-triazine (tptz),[Cu (tptz) 2] 2+: X-ray crystal structure, DNA binding and in vitro cell cytotoxicity. *Polyhedron, 44*(1), 101-112. doi: 10.1016/j.poly.2012.06.089

Abu, T., Ghithan, J., Darwish, S., & Abu-Hadid, M. M. (2012). Multi-Spectroscopic Investigation of the Interactions between Cholesterol and Human Serum Albumin. *Journal of Applied Biological Sciences, 6*(3), 45-55. Retrieved from www.nobel.gen.tr

Ahmadi, F., Alizadeh, A., Shahabadi, N., & Rahimi-Nasrabadi, M. (2011). Study binding of Al–curcumin complex to ds-DNA, monitoring by multispectroscopic and voltammetric techniques. *Spectrochimica Acta Part A: Molecular and Biomolecular Spectroscopy, 79*(5), 1466-1474. doi: 10.1016/j.saa.2011.05.002

Alagesan, M., Bhuvanesh, N., & Dharmaraj, N. (2014). Binuclear copper complexes: synthesis, X-ray structure and interaction study with nucleotide/protein by in vitro biochemical and electrochemical analysis. *European journal of medicinal chemistry, 78*, 281-293. doi: 10.1016/j.ejmech.2014.03.043

Aminzadeh, M., Mansouri-Torshizi, H., & Modarresi-Alam, A. R. (2016). 2, 2′-bipyridine coplanar with coordination square of Pd (II) nonyldithiocarbamato antitumor complex interacting with DNA in two distinct steps. *Journal of Biomolecular Structure and Dynamics*, 1-13. doi: 10.1080/07391102.2016.1220328

Anbazhagan, V., & Renganathan, R. (2008). Study on the binding of 2, 3-diazabicyclo [2.2. 2] oct-2-ene with bovine serum albumin by fluorescence spectroscopy. *Journal of Luminescence, 128*(9), 1454-1458. doi: 10.1016/j.jlumin.2008.02.004

Angelici, R. J. (1969). *Synthesis and techniques in inorganic chemistry*: Saunders.

Anjomshoa, M., Fatemi, S. J., Torkzadeh-Mahani, M., & Hadadzadeh, H. (2014). DNA-and BSA-binding studies and anticancer activity against human breast cancer cells (MCF-7) of the zinc (II) complex coordinated by 5, 6-diphenyl-3-(2-pyridyl)-1, 2, 4-triazine. *Spectrochimica Acta Part A: Molecular and Biomolecular Spectroscopy, 127*, 511-520. doi: 10.1016/j.saa.2014.02.048

Annaraj, B., Balakrishnan, C., & Neelakantan, M. (2016). Synthesis, structure information, DNA/BSA binding affinity and in vitro cytotoxic studies of mixed ligand copper (II) complexes containing a

phenylalanine derivative and diimine co-ligands. *Journal of Photochemistry and Photobiology B: Biology, 160*, 278-291. doi: 10.1016/j.jphotobiol.2016.04.021

Arnesano, F., Losacco, M., & Natile, G. (2013). An updated view of cisplatin transport. *European Journal of Inorganic Chemistry, 2013*(15), 2701-2711. doi: 10.1002/ejic.201300001

Ascenzi, P., & Fasano, M. (2010). Allostery in a monomeric protein: the case of human serum albumin. *Biophysical chemistry, 148*(1), 16-22. doi: 10.1016/j.bpc.2010.03.001

Baguley, B. C., & Le Bret, M. (1984). Quenching of DNA-ethidium fluorescence by amsacrine and other antitumor agents: a possible electron-transfer effect. *Biochemistry, 23*(5), 937-943. doi: 10.1021/bi00300a022

Banerjee, P., Ghosh, S., Sarkar, A., & Bhattacharya, S. C. (2011). Fluorescence resonance energy transfer: a promising tool for investigation of the interaction between 1-anthracene sulphonate and serum albumins. *Journal of Luminescence, 131*(2), 316-321. doi: 10.1016/j.jlumin.2010.10.022

Bi, S., Song, D., Tian, Y., Zhou, X., Liu, Z., & Zhang, H. (2005). Molecular spectroscopic study on the interaction of tetracyclines with serum albumins. *Spectrochimica Acta Part A: Molecular and Biomolecular Spectroscopy, 61*(4), 629-636. doi: 10.1016/j.saa.2004.05.028

Bobek, V., Pinterova, D., Kolostova, K., Boubelik, M., Douglas, J., Teyssler, P., . . . Kovarik, J. (2006). Streptokinase increases the sensitivity of colon cancer cells to chemotherapy by gemcitabine and cis-platine in vitro. *Cancer letters, 237*(1), 95-101. doi: 10.1016/j.canlet.2005.05.030

Budagumpi, S., Kulkarni, N. V., Kurdekar, G. S., Sathisha, M., & Revankar, V. K. (2010). Synthesis and spectroscopy of Co II, Ni II, Cu II and Zn II complexes derived from 3, 5-disubstituted-1H-pyrazole derivative: a special emphasis on DNA binding and cleavage studies. *European journal of medicinal chemistry, 45*(2), 455-462. doi: 10.1016/j.ejmech.2009.10.026

Chaveerach, U., Meenongwa, A., Trongpanich, Y., Soikum, C., & Chaveerach, P. (2010). DNA binding and cleavage behaviors of copper (II) complexes with amidino-O-methylurea and N-methylphenyl-amidino-O-methylurea, and their antibacterial activities. *Polyhedron, 29*(2), 731-738. doi: 10.1016/j.poly.2009.10.031

Cotton, A. F., Wilkinson, G., Bochmann, M., & Murillo, C. A. (1999). *Advanced inorganic chemistry*: Wiley.

da Silveira, V. C., Benezra, H., Luz, J. S., Georg, R. C., Oliveira, C. C., & da Costa Ferreira, A. M. (2011). Binding of oxindole-Schiff base copper (II) complexes to DNA and its modulation by the ligand. *Journal of Inorganic Biochemistry, 105*(12), 1692-1703. doi: 10.1016/j.jinorgbio.2011.09.016

Derakhshankhah, H., Saboury, A., Bazl, R., Tajmir-Riahi, H., Falahati, M., Ajloo, D., . . . Moosavi-Movahedi, A. (2012). Synthesis, cytotoxicity and spectroscopy studies of a new copper (II) complex: calf thymus DNA and T47D as targets. *Journal of the Iranian Chemical Society, 9*(5), 737-746. doi: 10.1007/s13738-012-0086-3

Divsalar, A., Razmi, M., Saboury, A. A., Mansouri-Torshizi, H., & Ahmad, F. (2015). Biological Evaluation of a New Synthesized Pt (II) Complex by Cytotoxic and Spectroscopic Studies. *Cell biochemistry and biophysics, 71*(3), 1415-1424. doi: 10.1007/s12013-014-0364-z

Divsalar, A., Saboury, A., Yousefi, R., Moosavi-Movahedi, A., & Mansoori-Torshizi, H. (2007). Spectroscopic and cytotoxic studies of the novel designed palladium (II) complexes: β-Lactoglobulin and K562 as the targets. *International journal of biological macromolecules, 40*(4), 381-386. doi: 10.1016/j.ijbiomac.2006.09.015

Edwards, I. R., & Aronson, J. K. (2000). Adverse drug reactions: definitions, diagnosis, and management. *The lancet, 356*(9237), 1255-1259. doi: 10.1016/S0140-6736(00)02799-9

El-Shahawi, M., Al-Jahdali, M., Bashammakh, A., Al-Sibaai, A., & Nassef, H. (2013). Spectroscopic and electrochemical characterization of some Schiff base metal complexes containing benzoin moiety. *Spectrochimica Acta Part A: Molecular and Biomolecular Spectroscopy, 113*, 459-465. doi: 10.1016/j.saa.2013.04.090

Erdogan, D. A., & Özalp-Yaman, Ş. (2014). Novel Pt (II) complexes containing pyrrole oxime; synthesis, characterization and DNA binding studies. *Journal of Molecular Structure, 1064*, 50-57. doi: 10.1016/j.molstruc.2014.02.005

Eslami Moghadam, M., Saidifar, M., Divsalar, A., Mansouri-Torshizi, H., Saboury, A. A., Farhangian, H., & Ghadamgahi, M. (2016). Rich spectroscopic and molecular dynamic studies on the interaction of cytotoxic Pt (II) and Pd (II) complexes of glycine derivatives with calf thymus DNA. *Journal of Biomolecular Structure and Dynamics, 34*(1), 206-222. doi: 10.1080/07391102.2015.1015056

Fox, K. (1997). Drug-DNA Interact. Protocols. *Methods in Mol. Biol*

Gaber, M., El-Ghamry, H., & Fathalla, S. (2015). Ni (II), Pd (II) and Pt (II) complexes of (1H-1, 2, 4-triazole-3-ylimino) methyl] naphthalene-2-ol. Structural, spectroscopic, biological, cytotoxicity, antioxidant and DNA binding. *Spectrochimica Acta Part A: Molecular and Biomolecular Spectroscopy, 139*, 396-404. doi: 10.1016/j.saa.2014.12.057

Ghani, N. T. A., & Mansour, A. M. (2012). Novel palladium (II) and platinum (II) complexes with 1H-benzimidazol-2-ylmethyl-N-(4-bromo-phenyl)-amine: structural studies and anticancer activity. *European journal of medicinal chemistry, 47*, 399-411. doi: 10.1016/j.ejmech.2011.11.008

Gumus, F., Eren, G. k. e., Açık, L., Celebi, A., Ozturk, F., Yılmaz, S. u. k., . . . Elmalı, A. (2009). Synthesis, cytotoxicity, and DNA interactions of new cisplatin analogues containing substituted benzimidazole ligands. *Journal of medicinal chemistry, 52*(5), 1345-1357. doi: 10.1021/jm8000983

Hannon, M. J. (2007). Metal-based anticancer drugs: from a past anchored in platinum chemistry to a post-genomic future of diverse chemistry and biology. *Pure and Applied Chemistry, 79*(12), 2243-2261. doi: 10.1351/pac200779122243

Heydari, A., & Mansouri-Torshizi, H. (2016). Design, synthesis, characterization, cytotoxicity, molecular docking and analysis of binding interactions of novel acetylacetonatopalladium (II) alanine and valine complexes with CT-DNA and BSA. *RSC Advances, 6*(98), 96121-96137. doi: 10.1039/C6RA18803F

Huang, B. X., Kim, H.-Y., & Dass, C. (2004). Probing three-dimensional structure of bovine serum albumin by chemical cross-linking and mass spectrometry. *Journal of the American Society for Mass Spectrometry, 15*(8), 1237-1247. doi: 10.1016/j.jasms.2004.05.004

Huheey, J. E., Keiter, E. A., & Keiter, R. L. (1983). *Inorganic chemistry: principles of structure and reactivity*: Harper & Row Philidelphia.

Hussein, B. H. (2011). Spectroscopic studies of 7, 8-dihydroxy-4-methylcoumarin and its interaction with bovine serum albumin. *Journal of Luminescence, 131*(5), 900-908. doi: 10.1016/j.jlumin.2010.12.021

Icsel, C., Yilmaz, V. T., Kaya, Y., Durmus, S., Sarimahmut, M., Buyukgungor, O., & Ulukaya, E. (2015). Cationic Pd (II)/Pt (II) 5, 5-diethylbarbiturate complexes with bis (2-pyridylmethyl) amine and terpyridine: Synthesis, structures, DNA/BSA interactions, intracellular distribution, cytotoxic activity and induction of apoptosis. *Journal of inorganic biochemistry, 152*, 38-52. doi: 10.1016/j.jinorgbio.2015.08.026

Iglesias, B. A., Barata, J. F., Pereira, P. M., Girão, H., Fernandes, R., Tomé, J. P., . . . Cavaleiro, J. A. (2015). New platinum (II)–bipyridyl corrole complexes: Synthesis, characterization and binding studies with DNA and HSA. *Journal of Inorganic Biochemistry, 153*, 32-41. doi: 10.1016/j.jinorgbio.2015.08.016

Islami-Moghaddam, M., Mansouri-Torshizi, H., Divsalar, A., & Saboury, A. (2009). Synthesis, characterization, cytotoxic and DNA binding studies of diimine platinum (II) and palladium (II) complexes of short hydrocarbon chain ethyldithiocarbamate ligand. *Journal of the Iranian Chemical Society, 6*(3), 552-569. doi: 10.1007/BF03246535

Jayanthi, E., Anusuya, M., Bhuvanesh, N., Khalil, K., & Dharmaraj, N. (2015). Synthesis and characterization of ruthenium (II) hydrazone complexes as anticancer chemotherapeutic agents: in vitro DNA/BSA protein binding and cytotoxicity assay. *Journal of Coordination Chemistry, 68*(20), 3551-3565. doi: 10.1080/00958972.2015.1077950

Jin, X.-D., Yang, Y., Jiang, Y., Han, X., Wan, X., Liu, D., . . . Chang, X. (2015). Synthesis, characterization and interaction with bovine serum albumin of cyclometallated Pd (II) complexes containing arylimine and salicylaldimine co-ligands. *Journal of Organometallic Chemistry, 791*, 24-33. doi: 10.1016/j.jorganchem.2015.04.050

Kashanian, S., Khodaei, M. M., & Pakravan, P. (2010). Spectroscopic studies on the interaction of isatin with calf thymus DNA. *DNA and cell biology, 29*(10), 639-646. doi: 10.1089/dna.2010.1054

Katrahalli, U., Jaldappagari, S., & Kalanur, S. S. (2010). Study of the interaction between fluoxetine hydrochloride and bovine serum albumin in the imitated physiological conditions by multi-

spectroscopic methods. *Journal of Luminescence, 130*(2), 211-216. doi: 10.1016/j.jlumin.2009.07.033

Katrahalli, U., Kalalbandi, V. K. A., & Jaldappagari, S. (2012). The effect of anti-tubercular drug, ethionamide on the secondary structure of serum albumins: a biophysical study. *Journal of pharmaceutical and biomedical analysis, 59*, 102-108. doi: 10.1016/j.jpba.2011.09.013

Khorasani-Motlagh, M., Noroozifar, M., & Mirkazehi-Rigi, S. (2010). Fluorescence and DNA-binding spectral studies of neodymium (III) complex containing 2, 2′-bipyridine,[Nd (bpy) 2 Cl 3· OH 2]. *Spectrochimica Acta Part A: Molecular and Biomolecular Spectroscopy, 75*(2), 598-603. doi: 10.1016/j.saa.2009.11.024

Khosravi, F., & Mansouri-Torshizi, H. (2017). Antibacterial combination therapy using Co3+, Cu2+, Zn2+ and Pd2+ complexes: Their calf thymus DNA binding studies. *Journal of Biomolecular Structure and Dynamics*, 1-20. doi: 10.1080/07391102.2017.1281171

Kostova, I. (2006). Platinum complexes as anticancer agents. *Recent patents on anti-cancer drug discovery, 1*(1), 1-22. doi: 10.2174/157489206775246458

Lakowicz, J. R., & Weber, G. (1973). Quenching of fluorescence by oxygen. Probe for structural fluctuations in macromolecules. *Biochemistry, 12*(21), 4161-4170. doi: 10.1021/bi00745a020

Li, G.-Y., Du, K.-J., Wang, J.-Q., Liang, J.-W., Kou, J.-F., Hou, X.-J., . . . Chao, H. (2013). Synthesis, crystal structure, DNA interaction and anticancer activity of tridentate copper (II) complexes. *Journal of inorganic biochemistry, 119*, 43-53. doi: 10.1016/j.jinorgbio.2012.09.019

Mansoori-Torshizi, H., Islami-Moghaddam, M., & Saboury, A. A. (2003). A microcalorimetry and spectroscopy study on the interaction of BSA with 2, 2'-bipyridine octylglycinato palladium (II) nitrate. *Sheng wu hua xue yu sheng wu wu li xue bao Acta biochimica et biophysica Sinica, 35*(10), 886-890. Retrieved from https://www.ncbi.nlm.nih.gov/pubmed/14515204

Mansouri-Torshizi, H., Eslami-Moghadam, M., Divsalar, A., & Saboury, A.-A. (2011). DNA-binding studies of some potential antitumor 2, 2'–bipyridine Pt (II)/Pd (II) complexes of piperidinedithiocarbamate. Their synthesis, spectroscopy and cytotoxicity. *Acta Chim Slov, 58*, 811-822. Retrieved from www.ncbi.nlm.nih.gov/pubmed/24061133

Mansouri-Torshizi, H., Mahboube, I., Divsalar, A., & Saboury, A.-A. (2008). 2, 2′-Bipyridinebutyldithiocarbamatoplatinum (II) and palladium (II) complexes: synthesis, characterization, cytotoxicity, and rich DNA-binding studies. *Bioorganic & medicinal chemistry, 16*(21), 9616-9625. doi: 10.1016/j.bmc.2008.08.021

Matei, I., Ionescu, S., & Hillebrand, M. (2011). Interaction of fisetin with human serum albumin by fluorescence, circular dichroism spectroscopy and DFT calculations: binding parameters and conformational changes. *Journal of Luminescence, 131*(8), 1629-1635. doi: 10.1016/j.jlumin.2011.03.073

Matesanz, A. I., & Souza, P. (2007). Palladium and platinum 3, 5-diacetyl-1, 2, 4-triazol bis (thiosemicarbazones): Chemistry, cytotoxic activity and structure–activity relationships. *Journal of inorganic biochemistry, 101*(2), 245-253. doi: 10.1016/j.jinorgbio.2006.09.024

Mohamed, M. S., Shoukry, A. A., & Ali, A. G. (2012). Synthesis and structural characterization of ternary Cu (II) complexes of glycine with 2, 2′-bipyridine and 2, 2′-dipyridylamine. The DNA-binding studies and biological activity. *Spectrochimica Acta Part A: Molecular and Biomolecular Spectroscopy, 86*, 562-570. doi: 10.1016/j.saa.2011.11.015

Montagner, D., Gandin, V., Marzano, C., & Longato, B. (2011). Synthesis, characterization and cytotoxic properties of platinum (II) complexes containing the nucleosides adenosine and cytidine. *Journal of inorganic biochemistry, 105*(6), 919-926. doi: 10.1016/j.jinorgbio.2011.03.009

Montana, A. M., & Batalla, C. (2009). The rational design of anticancer platinum complexes: the importance of the structure-activity relationship. *Current medicinal chemistry, 16*(18), 2235-2260. doi: 10.2174/092986709788453087

Mukherjee, T., Sen, B., Zangrando, E., Hundal, G., Chattopadhyay, B., & Chattopadhyay, P. (2013). Palladium (II) and platinum (II) complexes of deprotonated N, N′-bis (2-pyridinecarboxamide)-1, 2-benzene: Synthesis, structural characterization and binding interactions with DNA and BSA. *Inorganica Chimica Acta, 406*, 176-183. doi: 10.1016/j.ica.2013.04.033

Neault, J., & Tajmir-Riahi, H. (1998). Interaction of cisplatin with human serum albumin. Drug binding mode and protein secondary structure. *Biochimica et Biophysica Acta (BBA)-Protein Structure and Molecular Enzymology, 1384*(1), 153-159. doi: 10.1016/S0167-4838(98)00011-9

Niroomand, S., Khorasani-Motlagh, M., Noroozifar, M., & Moodi, A. (2012). Spectroscopic studies on the binding of holmium-1, 10-phenanthroline complex with DNA. *Journal of Photochemistry and Photobiology B: Biology, 117*, 132-139. doi: 10.1016/j.jphotobiol.2012.09.015

Ott, I., & Gust, R. (2007). Preclinical and clinical studies on the use of platinum complexes for breast cancer treatment. *Anti-Cancer Agents in Medicinal Chemistry (Formerly Current Medicinal Chemistry-Anti-Cancer Agents), 7*(1), 95-110. doi: 10.2174/187152007779314071

Özbek, N., Alyar, S., Alyar, H., Şahin, E., & Karacan, N. (2013). Synthesis, characterization and anti-microbial evaluation of Cu (II), Ni (II), Pt (II) and Pd (II) sulfonylhydrazone complexes; 2D-QSAR analysis of Ni (II) complexes of sulfonylhydrazone derivatives. *Spectrochimica Acta Part A: Molecular and Biomolecular Spectroscopy, 108*, 123-132. doi: 10.1016/j.saa.2013.01.005

Özdemir, Ü. Ö., Akkaya, N., & Özbek, N. (2013). New nickel (II), palladium (II), platinum (II) complexes with aromatic methanesulfonylhydrazone based ligands. Synthesis, spectroscopic characterization and in vitro antibacterial evaluation. *Inorganica Chimica Acta, 400*, 13-19. doi: 10.1016/j.ica.2013.01.031

Protogeraki, C., Andreadou, E. G., Perdih, F., Turel, I., Pantazaki, A. A., & Psomas, G. (2014). Cobalt (II) complexes with the antimicrobial drug enrofloxacin: Structure, antimicrobial activity, DNA-

and albumin-binding. *European journal of medicinal chemistry, 86*, 189-201. doi: 10.1016/j.ejmech.2014.08.043

Puthraya, K., Srivastava, T., Amonkar, A., Adwankar, M., & Chitnis, M. (1985). Some mixed-ligand palladium (II) complexes of 2, 2'-bipyridine and amino acids as potential anticancer agents. *Journal of inorganic biochemistry, 25*(3), 207-215. doi: 10.1016/0162-0134(85)80014-3

Raman, N., & Raja, J. S. (2007). DNA cleavage, structural elucidation and anti-microbial studies of three novel mixed ligand Schiff base complexes of copper (II). *Journal of the Serbian Chemical Society, 72*(10), 983-992. doi: 10.2298/JSC0710983R

Saeidifar, M., Mansouri-Torshizi, H., Palizdar, Y., Eslami-Moghaddam, M., Divsalar, A., & Saboury, A. A. (2014). Synthesis, characterization, cytotoxicity and DNA binding studies of a novel anionic organopalladium (II) complex. *Acta Chimica Slovenica, 61*(1), 126-136. Retrieved from www.dlib.si/details/URN:NBN:SI:DOC-ZJINWNR126

Shahraki, S., Mansouri Torshizi, H., Sori Nezami, Z., Ghahghaei, A., Yaghoubi, F., Divsalar, A., . . . H Shirazi, F. (2014). The effects of extending of co-planarity in a series of structurally relative polypyridyl Palladium (II) complexes on DNA-binding and cytotoxicity properties. *Iranian Journal of Pharmaceutical Research, 13*(4), 1279-1294. Retrieved from https://www.ncbi.nlm.nih.gov/pubmed/25587317

Shahraki, S., Shiri, F., Mansouri-Torshizi, H., & Shahraki, J. (2016). Characterization of the interaction between a platinum (II) complex and human serum albumin: spectroscopic analysis and molecular docking. *Journal of the Iranian Chemical Society, 13*(4), 723-731. doi: 10.1007/s13738-015-0784-8

Shaikh, S., Seetharamappa, J., Kandagal, P., & Manjunatha, D. (2007). In vitro study on the binding of anti-coagulant vitamin to bovine serum albumin and the influence of toxic ions and common ions on binding. *International journal of biological macromolecules, 41*(1), 81-86. doi: 10.1016/j.ijbiomac.2007.01.004

Shoukry, A. A., & Mohamed, M. S. (2012). DNA-binding, spectroscopic and antimicrobial studies of palladium (II) complexes containing 2, 2′-bipyridine and 1-phenylpiperazine. *Spectrochimica Acta Part A: Molecular and Biomolecular Spectroscopy, 96*, 586-593. doi: 10.1016/j.saa.2012.07.012

Singh, M. P., Joseph, T., Kumar, S., Bathini, Y., & Lown, J. W. (1992). Synthesis and sequence-specific DNA binding of a topoisomerase inhibitory analog of Hoechst 33258 designed for altered base and sequence recognition. *Chemical research in toxicology, 5*(5), 597-607. doi: 10.1021/tx00029a003

Sparks, J., & Scholz, C. (2009). Evaluation of a Cationic Poly (β-hydroxyalkanoate) as a Plasmid DNA Delivery System. *Biomacromolecules, 10*(7), 1715-1719. doi: 10.1021/bm900372x

Stanila, A., Nagy, C., Marcu, A., Cozma, D., Rusu, D., & David, L. (2009). Spectroscopic investigations of new metallic complexes with leucine as ligand. *Nuclear Instruments and Methods in Physics*

Research Section B: Beam Interactions with Materials and Atoms, 267(2), 419-421. doi: 10.1016/j.nimb.2008.10.024

Tabassum, S., Al-Asbahy, W. M., Afzal, M., & Arjmand, F. (2012). Synthesis, characterization and interaction studies of copper based drug with human serum albumin (HSA): spectroscopic and molecular docking investigations. *Journal of Photochemistry and Photobiology B: Biology, 114*, 132-139. doi: 10.1016/j.jphotobiol.2012.05.021

Wang, T., Xiang, B., Wang, Y., Chen, C., Dong, Y., Fang, H., & Wang, M. (2008). Spectroscopic investigation on the binding of bioactive pyridazinone derivative to human serum albumin and molecular modeling. *Colloids and Surfaces B: Biointerfaces, 65*(1), 113-119. doi: 10.1016/j.colsurfb.2008.03.008

Xu, Z.-H., Chen, F.-J., Xi, P.-X., Liu, X.-H., & Zeng, Z.-Z. (2008). Synthesis, characterization, and DNA-binding properties of the cobalt (II) and nickel (II) complexes with salicylaldehyde 2-phenylquinoline-4-carboylhydrazone. *Journal of Photochemistry and Photobiology A: Chemistry, 196*(1), 77-83. doi: 10.1016/j.jphotochem.2007.11.017

Yi, Y. W., & Bae, I. (2011). Effects of solvents on in vitro potencies of platinum compounds. *DNA repair, 10*(11), 1084-1085. doi: 10.1016/j.dnarep.2011.09.008

Yousefi, R., Mohammadi, R., Taheri-Kafrani, A., Shahsavani, M. B., Aseman, M. D., Nabavizadeh, S. M., . . . Moosavi-Movahedi, A.-A. (2015). Study of the interaction between two newly synthesized cyclometallated platinum (II) complexes and human serum albumin: Spectroscopic characterization and docking simulation. *Journal of Luminescence, 159*, 139-146. doi: 10.1016/j.jlumin.2014.10.055

Yue, Y., Chen, X., Qin, J., & Yao, X. (2009). Spectroscopic investigation on the binding of antineoplastic drug oxaliplatin to human serum albumin and molecular modeling. *Colloids and Surfaces B: Biointerfaces, 69*(1), 51-57. doi: 10.1016/j.colsurfb.2008.10.016

Zalba, S., & Garrido, M. J. (2013). Liposomes, a promising strategy for clinical application of platinum derivatives. *Expert opinion on drug delivery, 10*(6), 829-844. doi: 10.1517/17425247.2013.778240

Zhang, J., Li, L., Wang, L., Zhang, F., & Li, X. (2010). Synthesis, characterization and cytotoxicity of mixed-ligand complexes of palladium (II) with aromatic diimine and 4-toluenesulfonyl-L-amino acid dianion. *European journal of medicinal chemistry, 45*(11), 5337-5344. doi: 10.1016/j.ejmech.2010.08.058

Zhang, L.-W., Wang, K., & Zhang, X.-X. (2007). Study of the interactions between fluoroquinolones and human serum albumin by affinity capillary electrophoresis and fluorescence method. *Analytica chimica acta, 603*(1), 101-110. doi: 10.1016/j.aca.2007.09.021

(I)

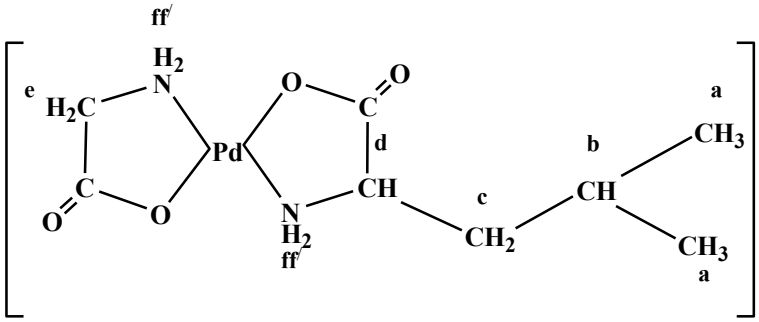

(II)

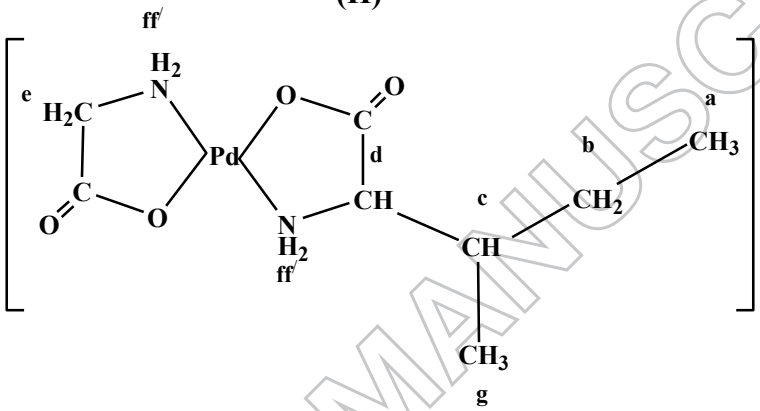

Fig. 1.

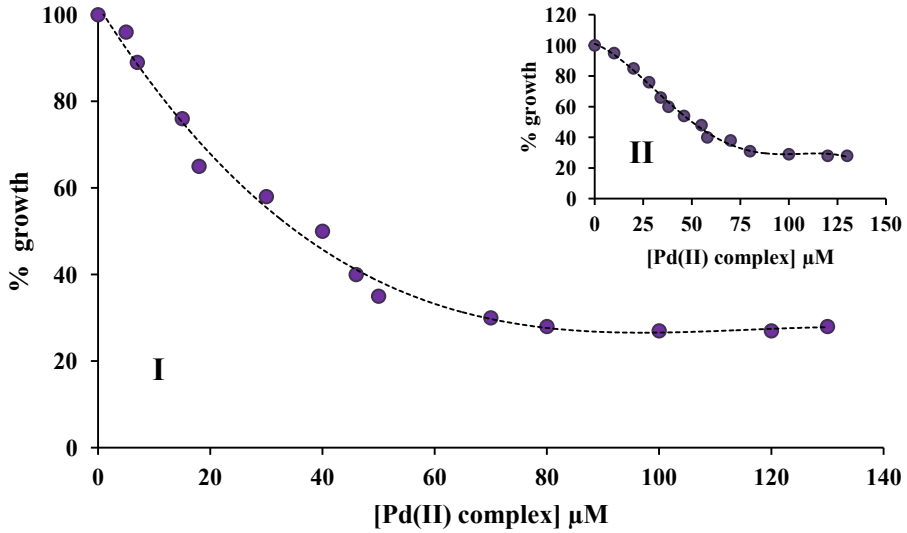

Fig. 2.

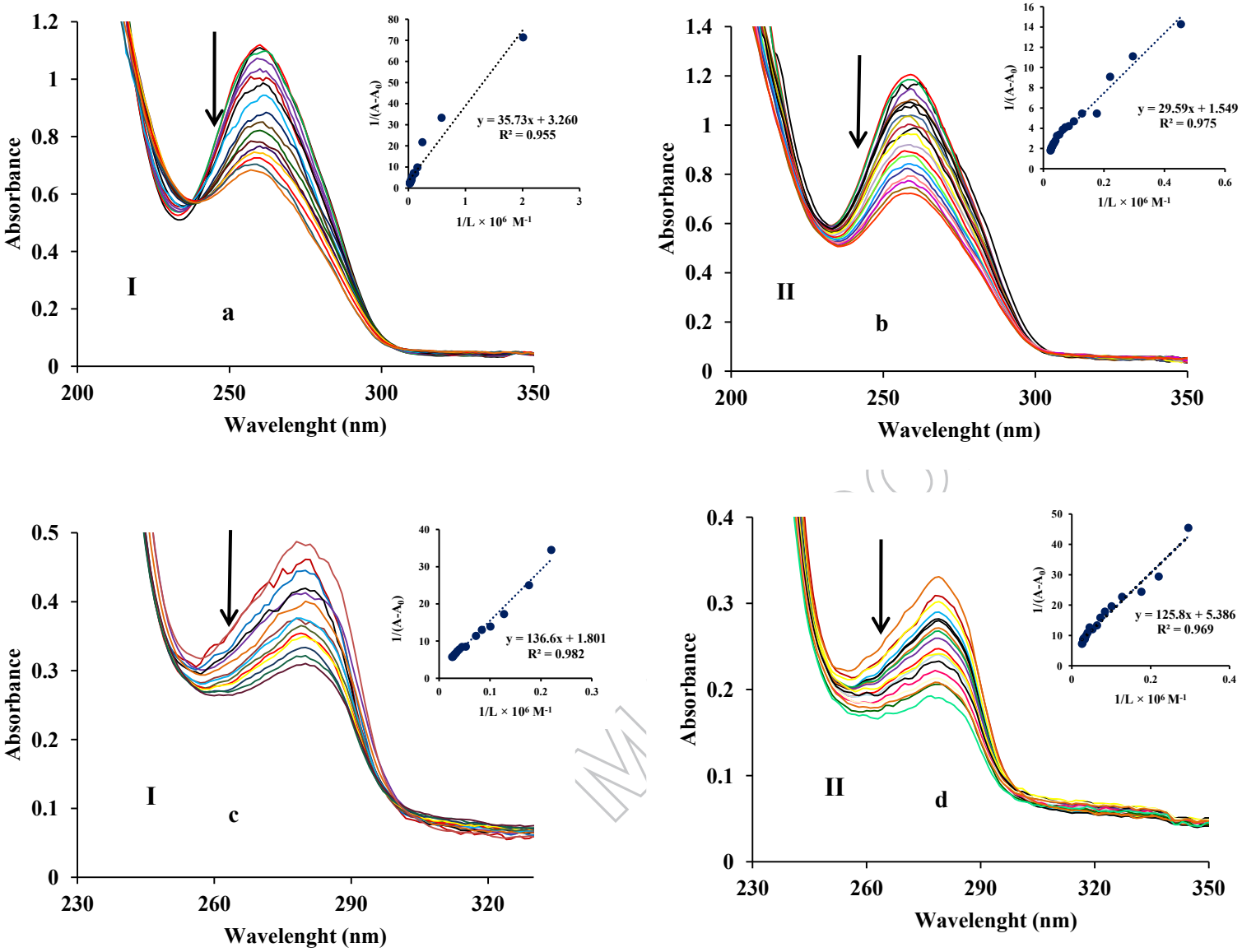

Fig.3.

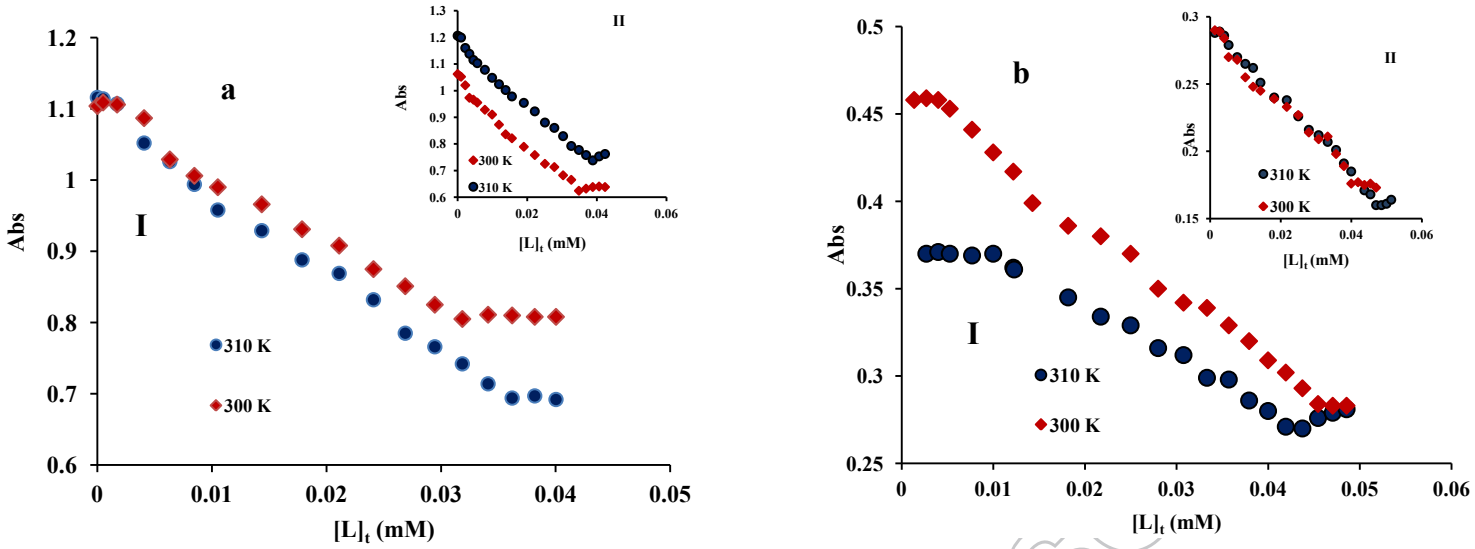

Fig.4

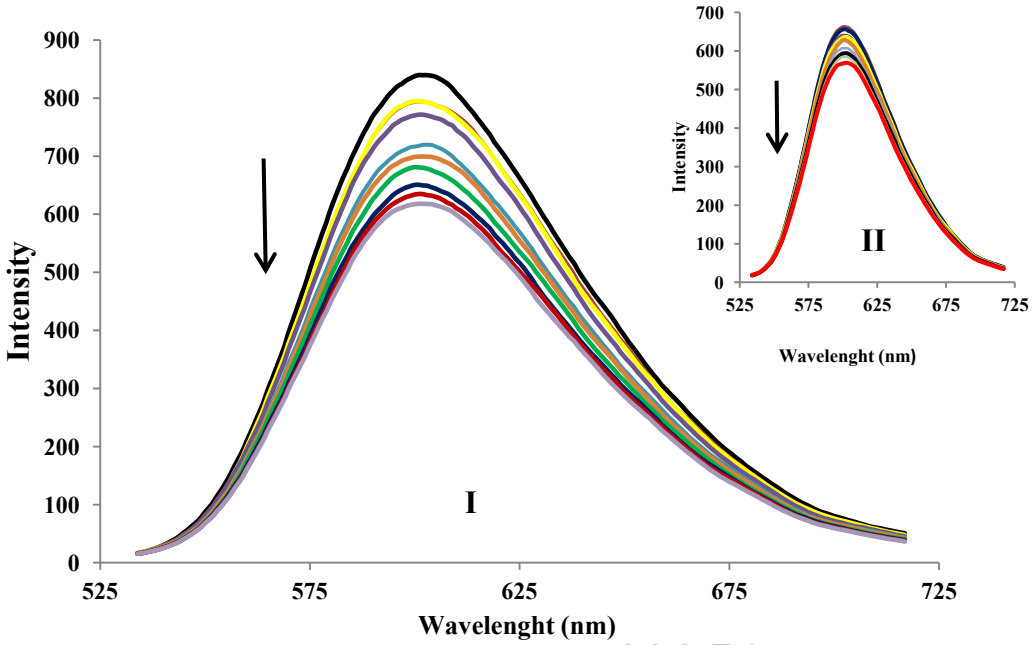

Fig.5.

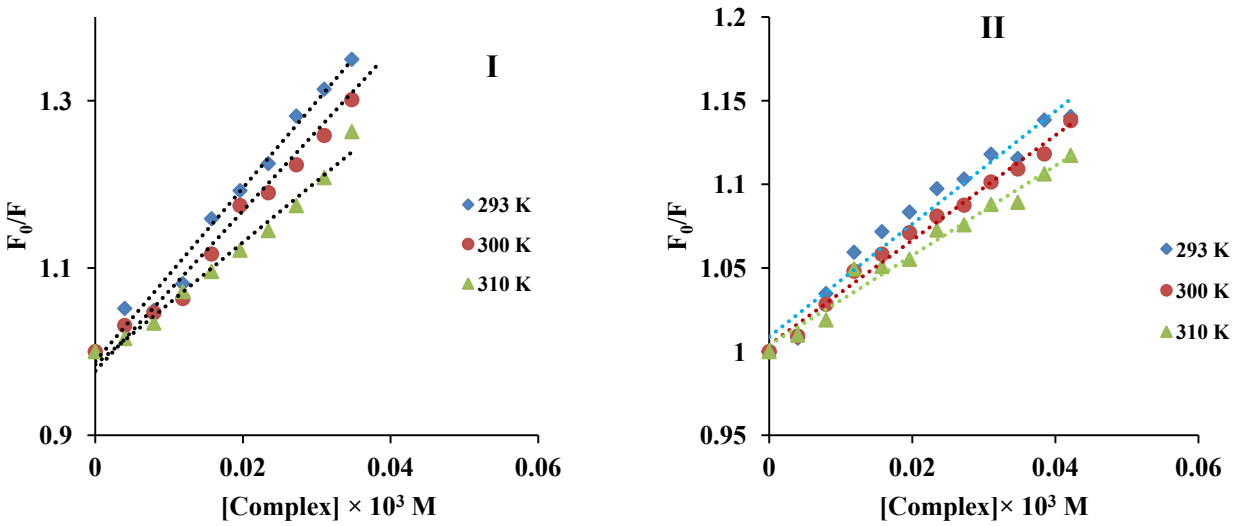

Fig. 6.

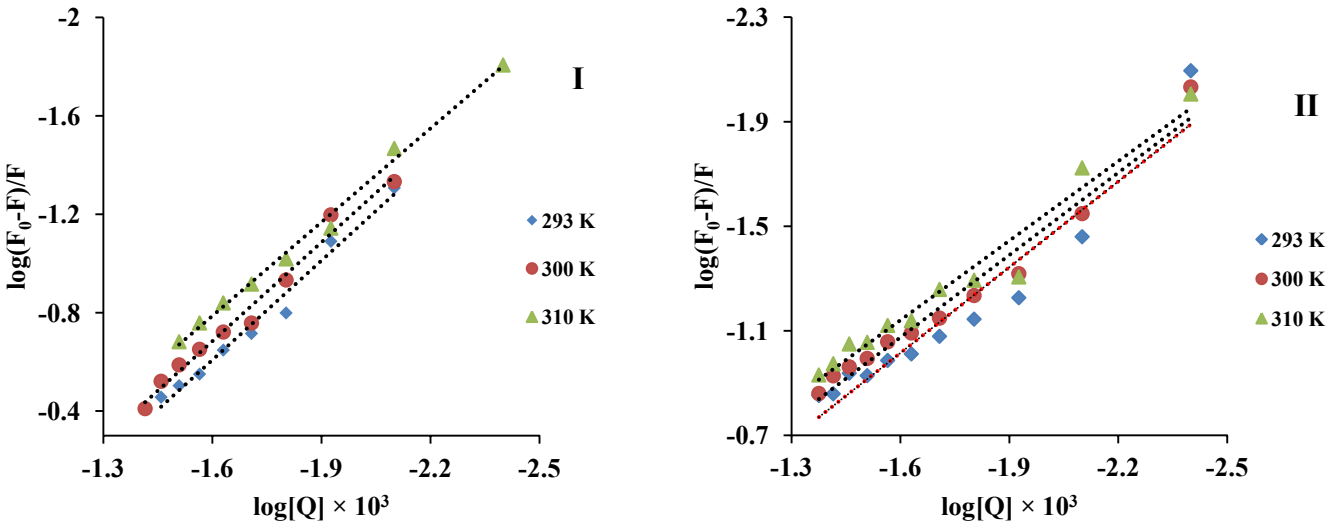

Fig. 7.

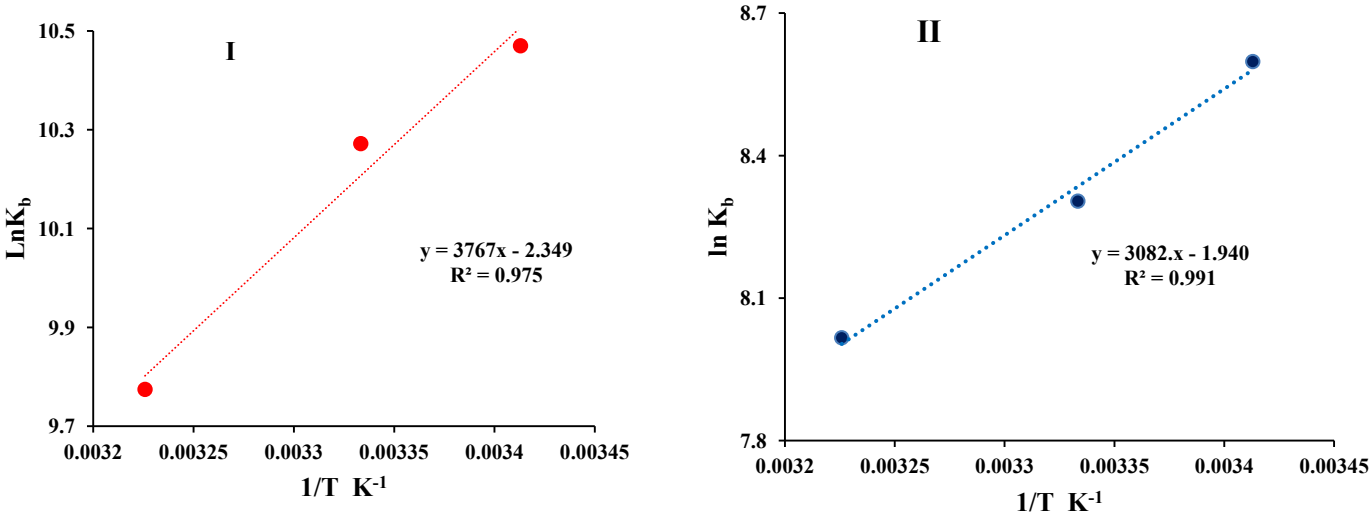

Fig.8.

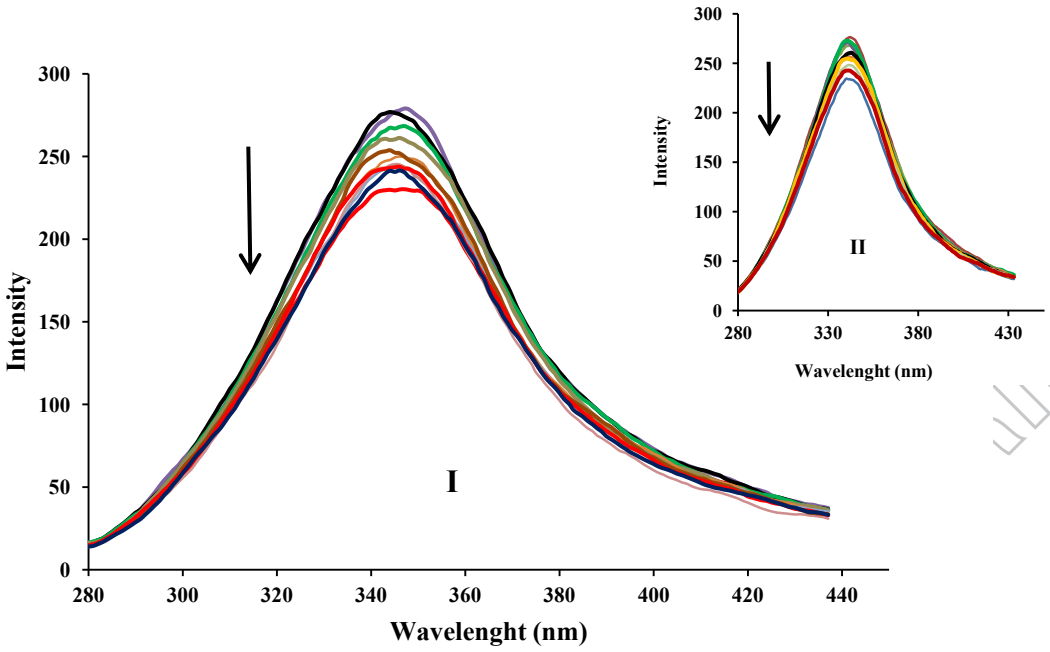

Fig. 9.

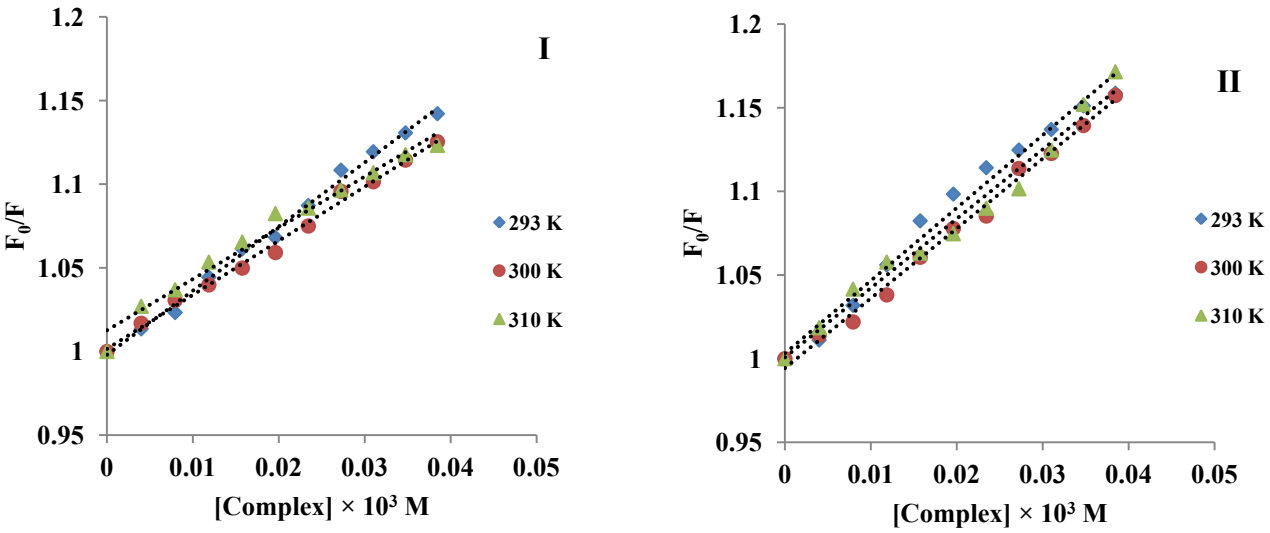

Fig. 10.

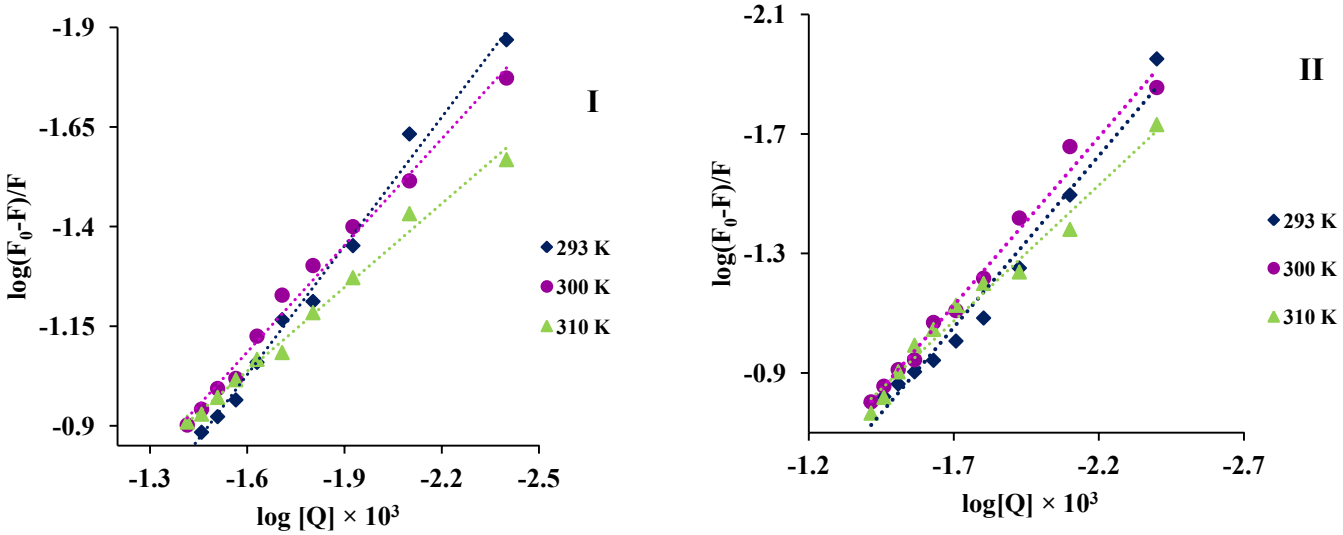

Fig. 11.

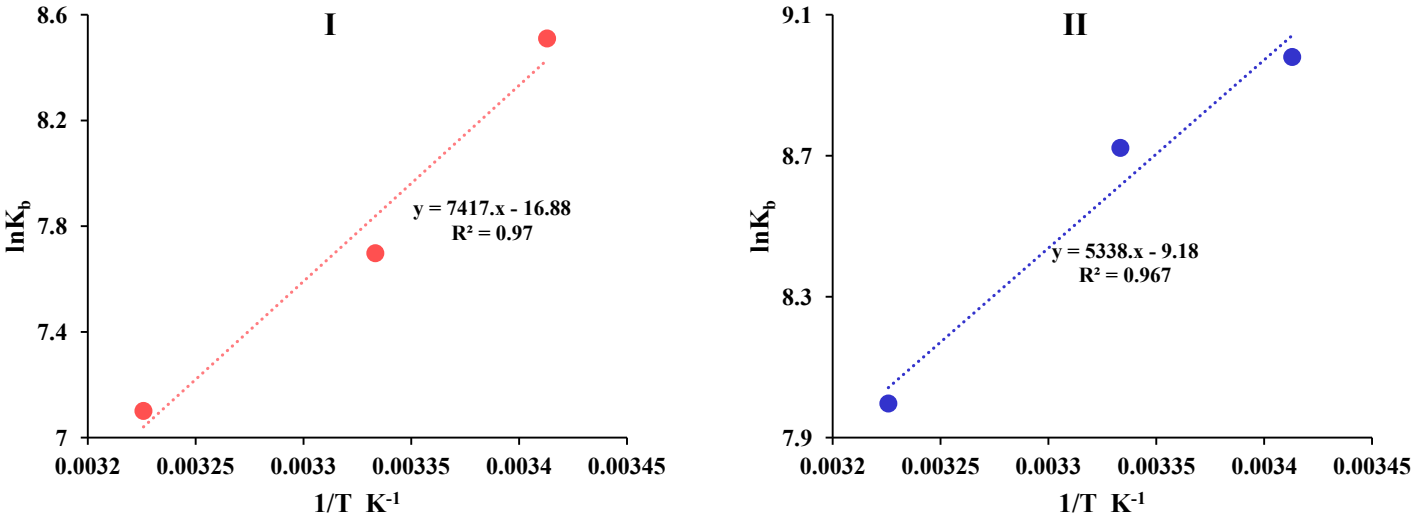

Fig. 12.

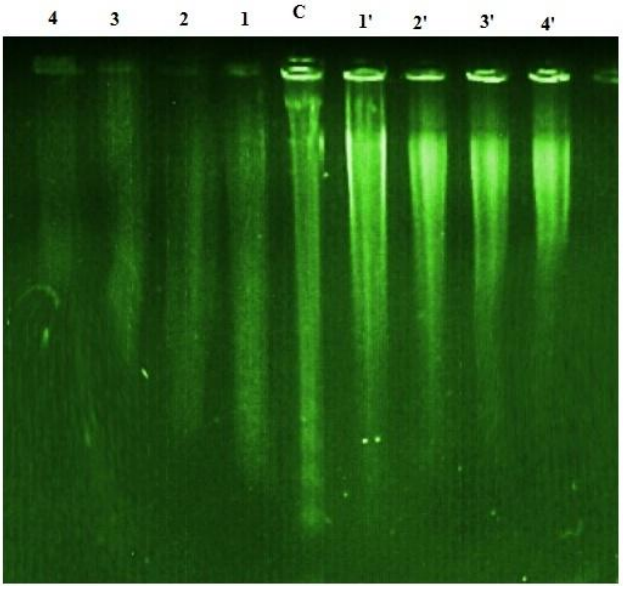

Fig. 13.

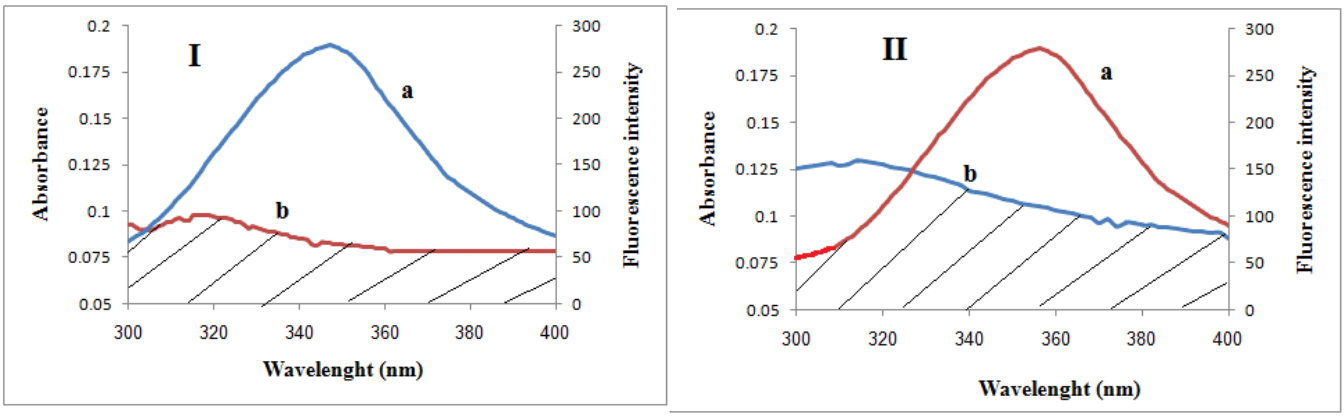

Fig. 14.

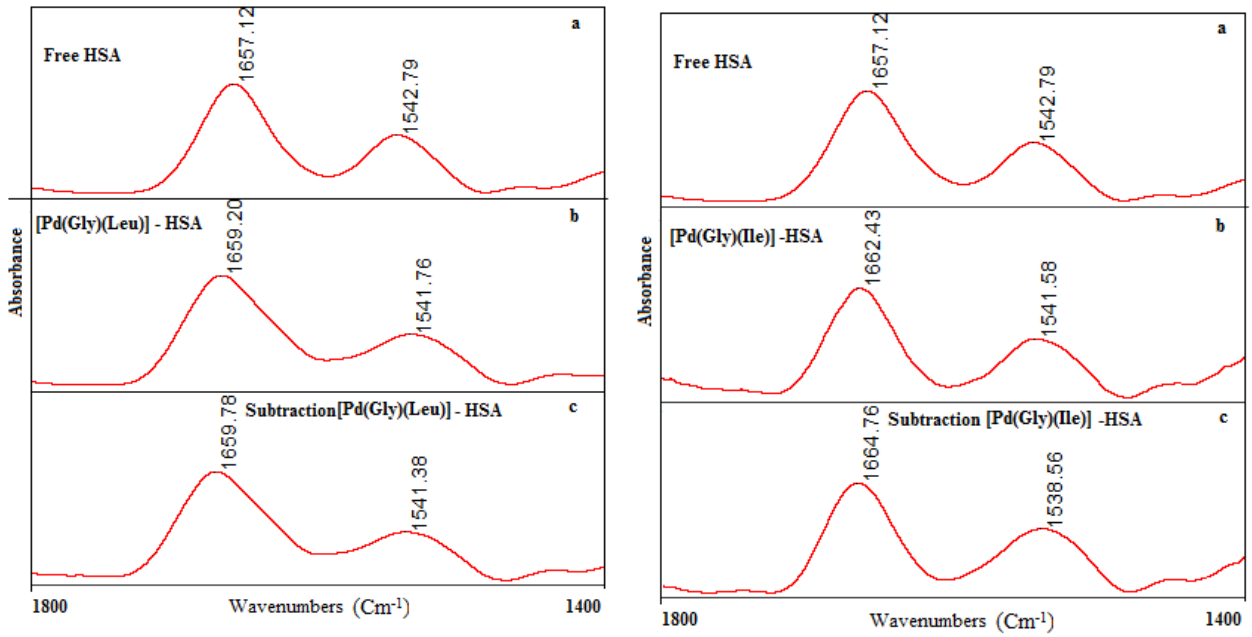

Fig. 15.

Figure Caption

Figure. 1. Proposed structures and numbering schemes of (**I**) [Pd(Gly)(Leu)] and (**II**) [Pd(Gly)(Ile)] Pd(II) complexes

Figure 2. The growth suppression activity of the complex **I** and inset complex **II** on K_{562} cell line were assessed using MTT assay. The tumor cells were incubated with varying concentrations of the complexes ranging from 0-100μM for 24h.

Figure 3. Effects of complexes **I** and **II** on the absorption spectrum of CT-DNA (a and b) and HSA(c and d) respectively. Inset; plot of 1/L vs. $1/(A-A_0)$ to give their corresponding K_{app} at 300K.

Figure 4. The changes of absorbance of DNA at λ_{max}=260nm (a) and HSA at λ_{max}=280nm (b) due to increasing the concentration of complexes **I** and **II**, at temperatures of 300 and 310K.

Figure 5. The emission spectra of CT-DNA-EB due to increasing the concentration of complexes **I** and **II**

Figure 6. The Stern–Volmer plots of the fluorescence titration of CT-DNA-EB with complexes **I** and **II**, at difference temperatures

Figure 7. Plot of $\log(F_0-F)/F$ versus log[Q] of CT-DNA interacted with complexes **I** and **II**, at difference temperatures

Figure 8. The Van't Hoff plot of complexes **I** and **II** with CT-DNA-EB at difference temperatures

Figure 9. The emission spectra of HSA due to increasing the concentration of complex **I**, inset complex **II**.

Figure 10. The Stern–Volmer plots of the fluorescence titration of HSA with complexes **I** and inset **II**, at difference temperatures

Figure 11. Plot of $\log(F_0-F)/F$ versus log[Q] of HSA interacted with complexes **I** and **II** at difference temperatures

Figure 12. The Van't Hoff plot of complexes **I** and **II** with HSA at difference temperatures

Figure 13. Agarose gel electrophoresis of CT-DNA samples showing the interaction between the two complexes **I** and **II** and CT-DNA in TAE buffer. Lane C: untreated CT-DNA. Lanes 1-4: 2.7mM CT-DNA + (1.25, 2.50, 3.75and 5.00mM) complex **I**. Lanes 1'- 4': 2.7mM CT-DNA + (1.25, 2.50, 3.75and 5.00mM) complex **II** respectively.

Figure 14. Spectral overlap of absorption spectra of complex **I** (b) and complex **II** (b) with fluorescence spectra of HSA alone(a). The ratio of Pd(II) complexes I and or II to HSA is 1:1 and equals 13μM.

Figure 15. FT-IR spectra and difference spectra of HSA in aqueous solution: (a)FT-IR spectrum of HSA; (b)FT-IR spectrum of Pd(II) complexes bounded to HSA; (c) FT-IR difference spectrum of HSA obtained by subtracting the spectrum of the Pd(II) complexes form from that of the Pd(II) complex bound form in the region of 1800–1400cm^{-1} Tris–HCl buffer (pH 7.0) ([HSA] = 0.003mM; [complex] = 0.003mM)

Table 1: Apparent constant and concentration of metal complexes in the midpoint of transition obtained from UV-Vis studies

Pd(II)complexes	DNA interaction			HSA interaction		
	T (K)	K_{app} (10^4 M^{-1})	$[L]_{1/2}$ (mM)	T (K)	K_{app} (10^4 M^{-1})	$[L]_{1/2}$ (mM)
I	300	9.12	0.017	300	1.30	0.025
	310	….	0.019	310	….	0.027
II	300	5.23	0.018	300	4.28	0.021
	310	….	0.020	310	….	0.025

Table 2. The K_{sv}, K_q, K_b and n values of Pd(II) complexes in the interaction with CT-DNA

Pd(II)complexes	T (K)	K_{sv}[a] (10^4 M^{-1})	k_q[b] (10^{12} $M^{-1}s^{-1}$)	K_b[c] (10^4 M^{-1})	n[d]
I	293	1.04	1.04	3.52	1.35
	300	0.96	0.96	2.89	1.34
	310	0.73	0.73	1.75	1.27
II	293	0.34	0.34	0.54	1.09
	300	0.31	0.31	0.40	1.05
	310	0.27	0.27	0.30	1.01

[a] K_{SV}= Stern- Volmer quenching constant

[b]k_q= Apparent biomolecular quenching constant

[c] K_b= Binding constant

[d]n= Number of binding sites on DNA

Table 3. The thermodynamic values of Pd(II) complexes in CT-DNA-EB interaction

Pd(II)complexes	T (K)	ΔH^o (KJ/mol)	ΔS^o (J/molK)	ΔG^o (KJ/mol)
I	293	- 31.26	- 19.49	- 25.55
	300			- 25.41
	310			- 25.22
II	293	- 25.62	- 16.13	- 20.89
	300			- 20.78
	310			- 20.62

Table 4. The K_{sv}, K_q, K_b and n values of Pd(II) complexes in the interaction with HSA

Pd(II)complexes	T (K)	K_{sv}[a] (10^4 M^{-1})	k_q[b] (10^{12} $M^{-1}s^{-1}$)	K_b[c] (10^4 M^{-1})	n[d]
I	293	0.38	0.38	0.49	1.07
	300	0.32	0.32	0.22	0.89
	310	0.30	0.30	0.12	0.70
II	293	0.43	0.43	0.79	1.14
	300	0.42	0.42	0.61	1.12
	310	0.41	0.41	0.29	0.90

[a] K_{SV}= Stern- Volmer quenching constant

[b]k_q= Apparent biomolecular quenching constant

[c] K_b= Binding constant

[d]n= Number of binding sites on HSA

Table 5. The thermodynamic values of Pd(II) complexes in HSA interaction

Pd(II)complexes	T (K)	ΔH^o (KJ/mol)	ΔS^o (J/molK)	ΔG^o (KJ/mol)
I	293	- 61.66	- 140.32	- 20.55
	300			- 19.56
	310			- 18.16
II	293	- 44.38	- 76.32	- 22.01
	300			- 21.48
	310			- 20.72

Table 6. The FRET parameters of Pd(II) complexes in HSA interaction

Pd(II)complexes	J (cm^3 L mol^{-1})	E	R_0 (nm)	r (nm)
I	1.48×10^{-14}	0.18	2.69	3.48
II	1.30×10^{-14}	0.20	2.63	3.32